การรีฟอร์มมิงด้วยคาร์บอนไดออกไซด์ร่วมกับการออกซิเดชันบางส่วนของมีเทน

ภายใต้การดำเนินงานแบบสับเปลี่ยนการป้อน

นางสาว สารินี เจริญเสรี

ลิขสิทธิ์ของจุฬาลงกรณ์มหาวิทยาลัย

COMBINED CARBON DIOXIDE REFORMING AND PARTIAL OXIDATION OF METHANE UNDER PERIODIC OPERATION

Miss Sarinee Charoenseri

A Thesis Submitted in Partial Fulfillment of the Requirements
for the Degree of Master of Engineering Program in Chemical Engineering
Department of Chemical Engineering
Faculty of Engineering
Chulalongkorn University
Academic Year 2007
Copyright of Chulalongkorn University

501844

Thesis Title	COMBINED CARBON DIOXIDE REFORMING AND PARTIAL OXIDATION OF METHANE UNDER PERIODIC OPERATION
By	Miss Sarinee Charoenseri
Field of Study	Chemical Engineering
Thesis Advisor	Associate Professor Suttichai Assabumrungrat, Ph.D.
Thesis Co-advisor	Assistant Professor Navadol Laosiripojana, Ph.D.

Accepted by the Faculty of Engineering, Chulalongkorn University in Partial Fulfillment of the Requirements for the Master's Degree
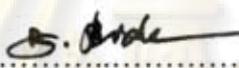
.... Dean of the Faculty of Engineering

(Associate Professor Boonsom Lerdhirunwong, Dr.Ing.)

THESIS COMMITTEE
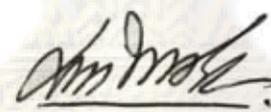
.... Chairman

(Associate Professor Supakanok Thongyai, Ph.D.)
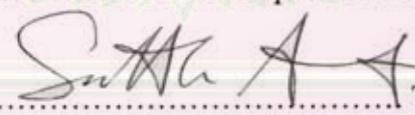
.... Thesis Advisor

(Associate Professor Suttichai Assabumrungrat, Ph.D.)

.... Thesis Co-advisor

(Assistant Professor Navadol Laosiripojana, Ph.D.)
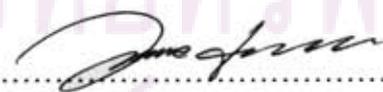
.... External Member

(Assistant Professor Worapon Kiatkittipong, D.Eng.)
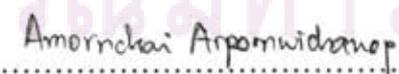
.... Member

(Assistant Professor Amornchai Arpornwichanop, D.Eng.)

iv

สารินี เจริญเสรี: การรีฟอร์มมิงด้วยคาร์บอนไดออกไซด์ร่วมกับการออกซิเดชันบางส่วนของมีเทนภายใต้การดำเนินงานแบบสับเปลี่ยนการป้อน (COMBINED CARBON DIOXIDE REFORMING AND PARTIAL OXIDATION OF METHANE UNDER PERIODIC OPERATION) อ. ที่ปรึกษา: รศ.ดร. สุทธิชัย อัสสะบำรุงรัตน์, 81 หน้า.

งานวิจัยนี้ทำการศึกษาสมรรถนะทางปฏิกิริยาเคมีของการรีฟอร์มมิงด้วยคาร์บอนไดออกไซด์ร่วมกับการออกซิเดชันบางส่วนของมีเทนภายใต้การดำเนินงานแบบสับเปลี่ยนการป้อนโดยใช้ตัวเร่งปฏิกิริยาโลหะนิกเกิลบนตัวรองรับซิลิกอนไดออกไซด์และแมกนีเซียมออกไซด์ จากการใช้เครื่องมือวิเคราะห์ต่าง ๆ ได้แก่ การวัดพื้นที่ผิวของตัวเร่งปฏิกิริยา สแกนนิงอิเลคตรอนไมโครสโคป การกระเจิงรังสีเอ็กซ์และการออกซิเดชันแบบโปรแกรมอุณหภูมิ เพื่อวิเคราะห์คุณลักษณะตัวเร่งปฏิกิริยาที่ผ่านการทำปฏิกิริยาพบว่า ปฏิกิริยานี้สามารถหยุดยั้งการสะสมของคาร์บอนที่เกิดขึ้นบนพื้นผิวของตัวเร่งปฏิกิริยาได้ และสามารถรักษาแอคติวิตีของตัวเร่งปฏิกิริยาให้คงที่ตลอดการสับเปลี่ยนสารตั้งต้นเป็นจำนวน 12 รอบที่อุณหภูมิปฏิกิริยา 650 และ 750 องศาเซลเซียส การรีเจนเนอเรชันตัวเร่งปฏิกิริยาเกิดได้อย่างสมบูรณ์ ที่อุณหภูมิและอัตราส่วนโดยโมลของออกซิเจนในสายป้อนสูง โดยพบคาร์บอนที่สะสมอยู่บนตัวเร่งปฏิกิริยาเพียงเล็กน้อย อย่างไรก็ตาม การเติมออกซิเจนส่งผลให้ค่าการเปลี่ยนของคาร์บอนไดออกไซด์ลดลง พบว่าสภาวะที่เหมาะสมของการดำเนินงานแบบสับเปลี่ยนการป้อนซึ่งให้ค่าสมรรถนะทางปฏิกิริยาเคมีสูงที่สุด คือ การใช้เวลา 5 นาที สำหรับการแตกตัวของมีเทน และ 5 นาที สำหรับการรีเจนเนอเรชันด้วยคาร์บอนไดออกไซด์และออกซิเจนในอัตราส่วนโดยโมล 9 ต่อ 1 ที่อุณหภูมิปฏิกิริยา 650 องศาเซลเซียส นอกจากนี้ยังพบว่าการดำเนินงานแบบสับเปลี่ยนการป้อนให้ค่าร้อยละผลได้ของไฮโดรเจนใกล้เคียงกับการดำเนินงานแบบไหลร่วมที่อุณหภูมิ 650 องศาเซลเซียส

ศูนย์วิทยทรัพยากร
จุฬาลงกรณ์มหาวิทยาลัย

ภาควิชา......วิศวกรรมเคมี........... ลายมือชื่อนิสิต.......สาริณี เจริญเสรี........
สาขาวิชา......วิศวกรรมเคมี........... ลายมือชื่ออาจารย์ที่ปรึกษา......................
ปีการศึกษา.......2550............... ลายมือชื่ออาจารย์ที่ปรึกษาร่วม...................

4970626321 : MAJOR CHEMICAL ENGINEERING
KEYWORDS: CARBON DIOXIDE REFORMING OF METHANE/ PERIODIC OPERATION/ COKE FORMATION/ CATALYST DEACTIVATION.

SARINEE CHAROENSERI: COMBINED CARBON DIOXIDE REFORMING AND PARTIAL OXIDATION OF METHANE UNDER PERIODIC OPERATION. THESIS ADVISOR: SUTTICHAI ASSABUMRUNGRAT, Ph.D., 81 pp.

This work investigates the catalytic performance under periodic operation for combined carbon dioxide reforming and partial oxidation of methane over an industrial steam reforming $Ni/SiO_2.MgO$ catalyst. Various analytical techniques including BET surface area measurement, SEM, XRD, and TPO were employed to characterize the spent catalysts. It was shown that this reaction was able to suppress carbonaceous deposition on catalyst surface at reaction temperatures of 650 and $750^{o}C$ without any significant loss of activity for 12 cracking/regeneration cycles. Carbon dioxide with oxygen could fully regenerate the catalyst when operating at high oxygen content and reaction temperature, thus a lesser amount of coke was observed. However, the addition of oxygen caused slightly decrease in carbon dioxide conversion. The optimal performance for periodic operation was found under the condition with 5 min of the cracking step followed by 5 min of the regeneration step at $650^{o}C$ with CO_2/O_2 ratio about 9/1. Additionally, it was found that the periodic operation provided the hydrogen yield close to that of the steady state operation at $650^{o}C$.

Department .....Chemical Engineering ...	Student's signature ..... สาริณี เหรัญเสรี
Field of Study ..Chemical Engineering.....	Advisor's signature ......
Academic year ....2007.................	Co advisor's signature ....

ACKNOWLEDGEMENTS

CONTENTS

LIST OF TABLES

LIST OF FIGURES

Figure   page

CHAPTER I
INTRODUCTION

1.1 Rationale

Carbon dioxide reforming of methane or methane dry reforming (Eq. 1.1) has received great attention nowadays because both methane and carbon dioxide are greenhouse gases which are utilized simultaneously for producing synthesis gas or syngas (mixture of hydrogen and carbon monoxide). This is considered to be green for environment. Traditionally, syngas has been produced either by gasification of coal or by steam reforming. The carbon dioxide reforming of methane is also attractive from that the produced syngas has lower H_2/CO ratios which is a preferable feed stock for Fischer–Tropsch syntheses, methanol and oxygenated compounds production than that conventional process.

$$CH_4 + CO_2 \rightarrow 2H_2 + 2CO \qquad \Delta H°_{298} = 247 \text{ kJ/mol} \qquad (1.1)$$

However, this process has not reached to industrial level because of many limitations as follows:

1) It is a highly endothermic reaction and thus requires a large amount of energy to proceed.
2) This reaction encounters a serious problem of catalyst deactivation due to carbon deposition.
3) The formation of unavoidable water as a side product resulting in reduction of the syngas selectivity and H_2/CO ratio.

In contrast, the partial oxidation of methane is a totally exothermic reaction. It produces syngas by two steps consisting of methane combustion (Eq. 1.2) and methane reforming (Eq. 1.3). Because the reaction rate of combustion reaction is much higher than reforming reaction, this may lead to hot spot which is the large temperature difference in catalyst bed and difficult to control particularly for large-scale operation.

$$CH_4 + 2O_2 \rightarrow CO_2 + 2H_2O \qquad \Delta H°_{298} = -802 \text{ kJ/mol} \qquad (1.2)$$

$$CH_4 + \tfrac{1}{2}O_2 \rightarrow CO + 2H_2 \qquad \Delta H°_{298} = -36 \text{ kJ/mol} \qquad (1.3)$$

In order to overcome the limitations and maintain their advantages. The coupling of endothemic carbon dioxide reforming with exothermic partial oxidation of methane appears to be a promising process that would have economic advantages and allow efficient heat management of the system. In this combined process, the various H_2/CO ratios can control for Fischer–Tropsch syntheses by changing the feed composition.

In certain applications, CO-free hydrogen is necessary for utilization in proton-exchange membrane (PEM) fuel cell. Although this combined process can produce hydrogen, the existed carbon oxides have to be removed for preventing the poison of electrocatalyst. An approach for eliminating the need of hydrogen separation from other gaseous products from the combined carbon dioxide reforming and partial oxidation of methane is to operate the reaction periodically by repeating two steps of the direct cracking of methane and catalyst regeneration alternately.

In thermal catalytic cracking step (Eq. 1.4), methane is converted to hydrogen and solid coke which causes the catalyst deactivation and plugging of the reactor. Thus, the regeneration step (Eqs. 1.5-1.7) is required for refreshing the catalyst via carbon oxidation by carbon dioxide and oxygen.

$$CH_4 \rightarrow C + 2H_2 \qquad \Delta H°_{298} = 75 \text{ kJ/mol} \qquad (1.4)$$

$$C + CO_2 \rightarrow 2CO \qquad \Delta H°_{298} = 171 \text{ kJ/mol} \qquad (1.5)$$

$$C + 1/2O_2 \rightarrow CO \qquad \Delta H°_{298} = -111 \text{ kJ/mol} \qquad (1.6)$$

$$CO + 1/2O_2 \rightarrow CO_2 \qquad \Delta H°_{298} = -270 \text{ kJ/mol} \qquad (1.7)$$

This operation also offers a potential benefit on the heat integration. The exothermic heat from the catalyst regeneration can supply for the endothermic catalytic cracking of methane.

The supported metal group VIII elements have been used for this reaction. These metals such as Ru, Rh, Pd, Ir and Pt showed better resistance to carbon deposition compared to nickel. However, nickel catalyst is much cheaper than those metals and widely used for CO-free hydrogen production.

In the previous study of our group (Promaros et al., 2005), we reported that the performance of periodic operation for the carbon dioxide reforming of methane over an industrial steam reforming $Ni/SiO_2.MgO$ catalyst was lower than that of the steady-state operation over all ranges of reaction time for both reaction temperatures of 650 and $750^{\circ}C$. Because deposited carbon was incompletely removed by carbon dioxide in the regeneration step. Therefore, the efficient process for carbon removal by oxygen addition is required to improve the catalytic activity and stability in further study.

This work studies the combined carbon dioxide reforming and partial oxidation of methane over industrial steam reforming $Ni/SiO_2.MgO$ catalyst under periodic and steady state operations at reaction temperatures of 650 and $750^{\circ}C$. The effect of oxygen contents on catalytic performance of the reaction under periodic operation is investigated and compared to those of steady state operation. In order to confirm the efficiency of this process, spent catalysts after exposure in reaction at different conditions were characterized by using various analytical methods including BET surface area measurement, SEM, XRD, and TPO. Additionally, their performance under periodic operation at different cycle periods and cycle splits are also determined and also compared with those from steady state operation.

CHAPTER II
THEORY

2.1 Reforming reaction

In the reforming technology, there are three major processes for hydrogen and synthesis gas production from methane as follows.

- Steam reforming

$$CH_4 + H_2O \rightarrow CO + 3H_2 \qquad \Delta H°_{298} = 206 \text{ kJ/mol} \qquad (2.1)$$

- Carbon dioxide reforming

$$CH_4 + CO_2 \rightarrow 2CO + 2H_2 \qquad \Delta H°_{298} = 261 \text{ kJ/mol} \qquad (2.2)$$

- Partial oxidation

$$CH_4 + \tfrac{1}{2} O_2 \rightarrow CO + 2H_2 \qquad \Delta H°_{298} = -36 \text{ kJ/mol} \qquad (2.3)$$

$$CH_4 + 2O_2 \rightarrow CO_2 + 2H_2O \qquad \Delta H°_{298} = -802 \text{ kJ/mol} \qquad (2.4)$$

Autothermal reforming of methane is a well-proven technology and has been used in ammonia and methanol plants. Compared to those main processes, autothermal reforming is low investment, flexible operation and sot-free operation, the main reactions of this process are

$$CH_4 + 2O_2 \rightarrow CO_2 + 2H_2O \qquad \Delta H°_{298} = -802 \text{ kJ/mol}$$

$$CH_4 + H_2O \rightarrow CO + 3H_2 \qquad \Delta H°_{298} = 206 \text{ kJ/mol}$$
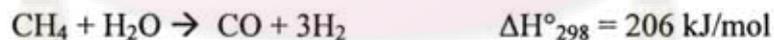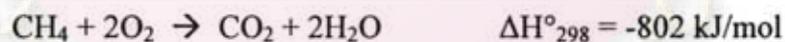
Recently, some attention has been paid to the carbon dioxide reforming and partial oxidation. Recent literatures have shown that combination of these reactions can effectively minimize the external energy requirements and reduce hot spots and carbon deposition on catalytic surface. Furthermore, by combining two reactions, the ratio of H_2/CO in product gas could be controlled to a desired level. Therefore, this process is a promising technology for converting two green house gases into other products.

2.1.1 Thermodynamics of carbon dioxide reforming of methane

The carbon dioxide reforming reaction has similar thermodynamic and equilibrium characteristics to steam reforming reaction. However, it generates syngas with lower H_2/CO ratio.

$$CH_4 + CO_2 \rightarrow 2CO + 2H_2 \qquad \Delta H^\circ_{298} = 261 \text{ kJ/mol} \qquad (2.5)$$

$$CH_4 + H_2O \rightarrow CO + 3H_2 \qquad \Delta H^\circ_{298} = 206 \text{ kJ/mol} \qquad (2.6)$$

The carbon dioxide reforming of methane is conducted under conditions where carbon formation via catalytic cracking of methane (Eq. 2.7) and/or Boudouard reaction (Eq. 2.8) is thermodynamically feasible.

$$CH_4 \rightarrow C + 2H_2 \qquad \Delta H^\circ_{298} = 75 \text{ kJ/mol} \qquad (2.7)$$

$$2CO \rightarrow C + CO_2 \qquad \Delta H^\circ_{298} = -171 \text{ kJ/mol} \qquad (2.8)$$

Other reactions which could also have an important influence on the overall product are:

$$CO_2 + H_2 \rightarrow CO + H_2O \qquad \Delta H^\circ_{298} = 40 \text{ kJ/mol} \qquad (2.9)$$

$$C + H_2O \rightarrow CO + H_2 \qquad \Delta H^\circ_{298} = 131 \text{ kJ/mol} \qquad (2.10)$$

Theoretically, the carbon formed in reaction (2.7) should be rapidly consumed by the reverse of reaction (2.8), and by the steam/carbon gasification reaction (2.10).

Practically, steam is almost always formed via the reverse water gas-shift (RWGS) reaction (2.9). Serious coke deposition on catalytic surface can be reduced by these two reactions. If the cracking reaction is faster than the carbon removal rate, there is formation of solid carbon, leading to catalyst deactivation and plugging problem in the reactor. However, it should be noted that the formation of water is not desired in this reaction system because it decreases the selectivity of hydrogen.

2.1.2 Reaction mechanism of carbon dioxide reforming of methane

Many researches have been attempted to clarify the reaction mechanism in the carbon dioxide reforming of methane. The possible mechanism of this reaction over supported metal catalyst was proposed by Solymosi *et al.* (1991, 1993). The dissociation of methane with activation carbon formed at the end of reaction would produce activation of methane as follows:

$$CH_4 \rightarrow CH_3^{\bullet} + H^{\bullet}, \tag{2.11}$$
$$CH_3^{\bullet} \rightarrow CH_2^{\bullet} + H^{\bullet}, \tag{2.12}$$
$$CH_2^{\bullet} \rightarrow CH^{\bullet} + H^{\bullet}, \tag{2.13}$$
$$CH^{\bullet} \rightarrow C^{\bullet} + H^{\bullet}. \tag{2.14}$$
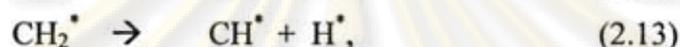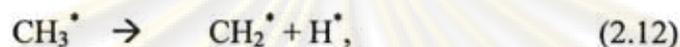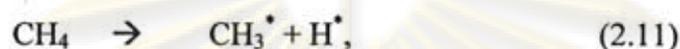
In general, there are many forms of deposited carbons, which are different in reactivity, i.e., adsorbed atomic carbon which is a highly reactive form, amorphous carbon, vermicular carbon, bulk nickel carbide, and crystalline graphitic carbon. The reactivity of deposited carbon depends on the type of catalytic surface, the temperature of its formation and the duration of thermal treatment. The formation of carbon from carbon monoxide with the precursor is shown by reaction (2.16).

$$CO_2 \rightarrow CO^{\bullet} + O^{\bullet}, \tag{2.15}$$
$$CO^{\bullet} \rightarrow C^{\bullet} + O^{\bullet}. \tag{2.16}$$
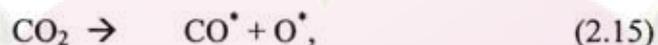
Unless both methane and carbon dioxide can dissociate separately, their deposited products terminate the respective dissociation by covering the metal surfaces. The self-decomposition of both methane and carbon dioxide could be facilitated via reactions (2.17)-(2.19). The dissociation of methane is enhanced by adsorbed oxygen, while the dissociation of carbon dioxide is also promoted by adsorbed hydrogen and other methane residues. Therefore, the reactions of these surface species also need to be considered as the following reactions:

$$CO_2 + H^{\bullet} \rightarrow CO^{\bullet} + OH^{\bullet}, \tag{2.17}$$
$$CH_4 + O^{\bullet} \rightarrow CH_3^{\bullet} + OH^{\bullet}, \tag{2.18}$$

$$CH_x + O^\bullet \quad \rightarrow \quad CH_3^\bullet + OH^\bullet, \qquad (2.19)$$

$$2OH \quad \rightarrow \quad H_2O^\bullet + O^\bullet. \qquad (2.20)$$
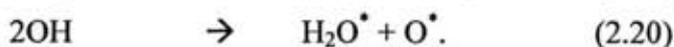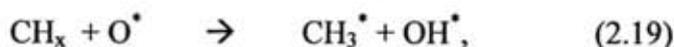
2.1.3 Thermodynamics of combined carbon dioxide reforming and partial oxidation of methane

The combined process of carbon dioxide reforming and partial oxidation of methane is a complex multi-reaction network system consisting of various major reactions as summarized below:

$$CH_4 + \tfrac{1}{2} O_2 \quad \rightarrow \quad CO + 2H_2 \qquad \Delta H^\circ_{298} = -36 \ kJ/mol$$

$$CH_4 + 2O_2 \quad \rightarrow \quad CO_2 + 2H_2O \qquad \Delta H^\circ_{298} = -802 \ kJ/mol$$

$$CH_4 + CO_2 \quad \rightarrow \quad 2CO + 2H_2 \qquad \Delta H^\circ_{298} = 261 \ kJ/mol$$

$$CH_4 + H_2O \quad \rightarrow \quad CO + 3H_2 \qquad \Delta H^\circ_{298} = 206 \ kJ/mol$$

$$CO_2 + H_2 \quad \rightarrow \quad CO + H_2O \qquad \Delta H^\circ_{298} = 206 \ kJ/mol$$
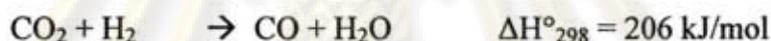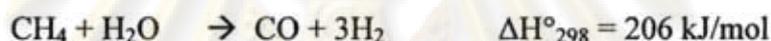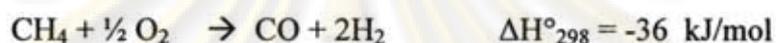
This process can produce syngas with H_2/CO ratios around 1, which is suitable for production of oxygenated compounds, heavy hydrocarbons by Fischer-Tropsch synthesis and carbon monoxide for synthesis of polycarbonates. Addition of oxygen feed to the carbon dioxide reforming can reduce the carbon deposition on the catalytic surface and increase methane conversion, although this can also cause the reduction of process selectivity. Moreover, as the methane oxidation is highly exothermic, the temperature control of the reactor may be very difficult at certain conditions, leading to the formation of hot spots. Addition of carbon dioxide feed to the partial oxidation reaction can improve the reactor temperature control and reduce the formation of hot spots.

2.1.4 Mechanism of Carbon Formation

In many processes, the formation of carbon on catalytic surface is an important problem. This may cause deactivation of the catalyst, blocking of catalyst pores and voids, or also physical properties of the catalyst support.

During the reaction, various types of carbon may be formed on nickel catalyst, two main types of deposited carbon, encapsulate and whisker carbons, are formed. The mechanism of carbon formation has been constructed on the basis of following steam reforming mechanism:

$$CO_2 \rightarrow CO + O_{Ad-metal} \qquad (2.21)$$

$$CO_2 \rightarrow CO + O_{Ad-sup\,port} \qquad (2.22)$$

$$CH_4 \rightarrow CH_{x-metal} + (4-x)/2H_2 \qquad (2.23)$$

$$CH_{x-metal} + O_{Ad-metal} \rightarrow x/2H_2 + CO \qquad (2.24)$$

$$CH_{x-metal} + O_{Ad-sup\,portl} \rightarrow x/2H_2 + CO \qquad (2.25)$$
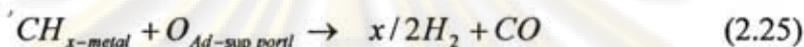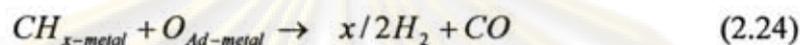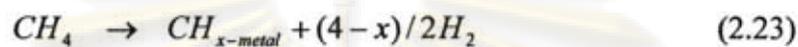
Figure 2.1 shows the mechanism of carbon formation. Two types of active sites are proposed on the catalyst, the one interacts with the catalyst support, the other at the surface of bulk nickel. Carbon deposited on the surface of bulk nickel is assembled to form carbon whiskers with nickel growing on top. If the nickel in the growing core can only be removed, carbonaceous deposition is suppressed without any deactivation of catalyst because the nickel on support which mainly participates in the reforming reaction is not detached.
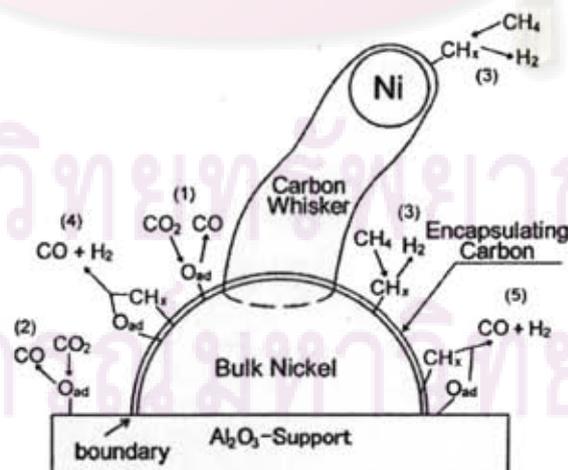
Figure 2.1 Model of reforming reaction and carbonaceous reaction (Ito, 1999)

For the surface reactions, the methane cracking or the Boudouard reaction produce adsorbed carbon atoms. Most carbon in catalytic cracking of methane is filamentous carbon. The surface carbon atoms would dissolve into the nickel particle at the gas side, and diffuse to the support side. A selvedge with high concentration is created at top of the nickel particle, because the surface is enriched with carbon, and the carbon concentration decreases from the surface concentration to the bulk concentration of interstitially dissolved carbon over a number of atomic layers.

The driving force for the bulk diffusion of carbon through the metal particle is described either to a temperature gradient (Baker et al., 1972; Yang et al., 1989) or to a concentration gradient (Rostrup-Nielsen et al., 1977; Kock et al., 1985; Alstrup et al., 1988). The filamentous carbon will be formed by the formation of a solution of carbon in nickel that is saturated with respect to filamentous carbon. The degree of saturation is determined by the affinity for carbon formation of the gas phase, it was experimentally observed that the formation of filamentous carbon is much more difficult under conditions with a low affinity for carbon formation. A slow nucleation occurs at low temperature and low gas phase concentration of methane, very long periods of increasing rate of carbon formation, and also a small number of carbon filaments that are able to nucleate under these conditions.

2.2 Periodic operation

The periodic operation refers to an operation in which one or more inputs into a chemical reactor vary with time, but each input is revisited after a time corresponding to the period. A typical example of the periodic operation of a reactor is shown in Figure 2.2. Two inputs with two volumetric flow rates of reactants 'A' and 'B' are switched periodically between two values. The chain of step-changes is generated representing a square-wave variation of reactant concentrations in the reactor feed. In most systems, the flow rate variations are matched such that the space velocity in the reactor remains constant. However, other inputs may be varied such as reactor temperature, flow rate, and flow direction.
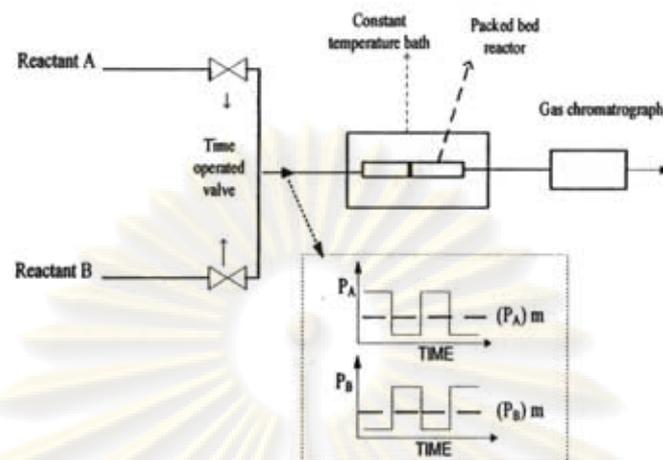
Figure 2.2 Schematic diagram of periodically operating reactor for two feed streams

Comparison between periodic operation and steady-state operation is shown in Figure 2.3. Input variations result in a time-varying output shown in the upper right of the figure. These are referred to instantaneous concentrations, yields, or rates. The more important information is the mean or time-average production rate, and yield or product concentration.
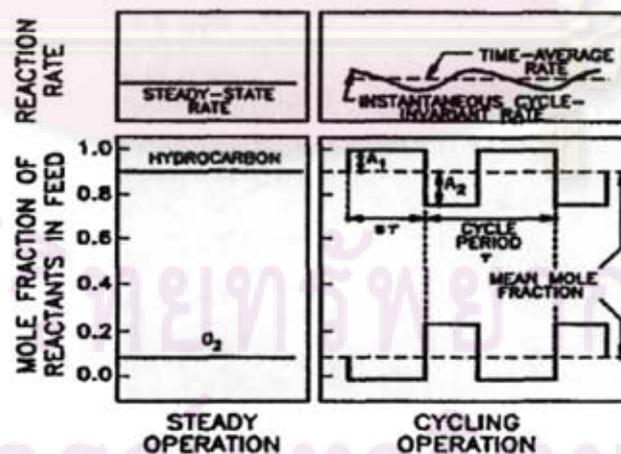
Figure 2.3 Comparison of steady state (left side) and periodic (right side) operation showing definition of the cycling variables: cycle period (frequency), r, cycle split (duty fraction), s; amplitudes, A_1, A_2. (Silveston, 1995)

Additionally, there are some variables to be introduced for periodic operation:

Period (τ)   -- the time between repetitions of a change in an input condition;

Split (s)   -- the duration of one part of cycle relative to the period;

Amplitude (A) -- the change in the value of an input condition between its highest and mean values.

The split at the value of 0.5 indicates a symmetrical cycle with both parts of equal duration. Split must be defined relative to one of the reactants. The split measures the relative duration of the portion of the cycle in which that reactant is at its highest concentration. Amplitude takes on just a single value for symmetrical forcing. However, other split values need to keep the space velocity in the reactor remains constant, two amplitude values must be given, one for each portion of the cycle.

Another variable is the phase lag. The composition changes shown in Figure 2.3 are 180 ° or ¶ radians out-of-phase. Other phase lags could be used such as in a pulsing operation, the phase lag is zero. In principle, temperature, pressure, or even flow velocity could be varied. The choice of inputs, mode of variation, and cycle structure are depend on the strategy.

The advantages of periodic operation could be summarized as follows:

- Increased catalyst activity, expressed as conversion or rate of reaction, especially for reactions in which conversion per pass is limited, often by equilibrium.
- Periodic operation may be a mean of permitting reactors to operate safely in regions of high parametric sensitivity such as in exothermic reaction.
- Controlling of catalyst deactivation could be attainable by forced modulation. There is evident that periodic operation can decrease the rate of catalyst deactivation.

For strategy in periodic operations, there are many ways for operating a reactor periodically. At least two components are required for composition

modulation. This limiting case, shown as two reactant cycles in Figure 2.4, presents two strategy options from a study of methanol synthesis. Moreover, there is an alternative to operate by varying any periodical variables, such as, period and split of each cycle for investigation the optimizing of scoped reaction. Furthermore, multi-part cycles are possible. Multi-part cycles could be useful in some circumstances, such as flushing the catalyst surface by inert gas to desorbed reactant or product before exposing the surface to a second reactant, as be showed in Figure 2.5
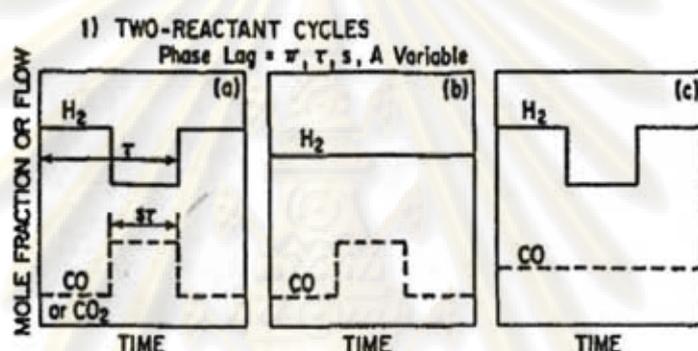
Figure 2.4 Different possible composition forcing operations with two components (reactants and/ or diluents) for methanol synthesis (Chanchlani, 1994).
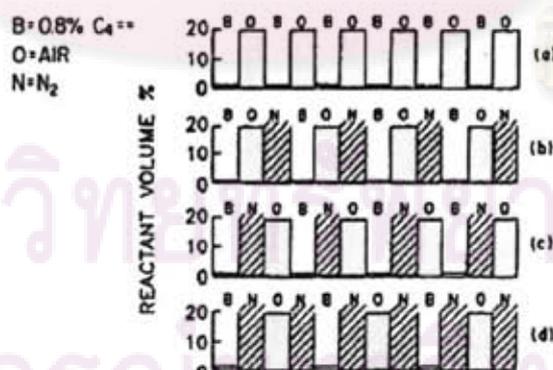
Figure 2.5 Modulation strategies with two-, three-, and four-part cycles for partial oxidation of butadiene to maleic anhydride with and without diluent flushing (Lang, 1991).

CHAPTER III
LITERATURE REVIEWS

Some recent researches have been concentrated on combined carbon dioxide reforming and partial oxidation of methane in synthesis gas production for several reasons. Firstly, the raw material of this process is available from abundant natural gas. Secondly, the ratio of H_2/CO in product gas could be controlled to a satisfied value by changing the feed composition. Thirdly, this reaction allows efficient heat management between endothermic and exothermic reactions. Finally, addition of oxygen into carbon dioxide reforming of methane can reduce the deposited carbon on catalytic surface. Many researches have been carried out on the development of effective catalysts and supports for carbon dioxide reforming of methane and their operating condition. However, only a few studies have focused on the new alternative of the periodic operation.

3.1 Effects of types of catalyst and support on carbon dioxide reforming of methane

Carbon dioxide reforming of methane was first studied by Fischer and Tropsch (1928) over various base metal catalysts. For industrial level, this reaction with excess carbon dioxide was applied for the Calcor process by using nickel based catalyst (Teuner *et al.*, 1985; Kurz *et al.*, 1990).

Nobel metals such as Pt, Pd and especially Rh have been reported to be active for dry reforming. Richardson *et al.* (1990) and Basini *et al.* (1991) revealed that Rh is a preferable element for carbon-free production because it gave methane and carbon dioxide conversion near equilibrium over a wide range of space velocity and gave high H_2 selectivity. Rostrup-Nielsen and Bak Hansen (1993) showed the reactivity order of supported group VIII elements to be Ru > Rh > Ni ≈ Ir > Pt > Pd. This is similar to the proposed order for steam reforming, indicating a similar mechanism of the two cases.

However, these noble metals are too expensive for practically utilization. Other metals such as Fe, Co and Ni are also known to be active for the reaction. Among them, Ni is the most promising for industrial application but the conventional Ni-based catalyst was reported to be sensitive for coking deposition. Therefore, many researchers have been currently carried out to improve the performance and lifetime of Ni-based catalyst.

Several Ni catalysts with long life and high activities have been reported in many literatures. These include Ni/Al_2O_3 (Takano et al., 1994,1996; Ito et al., 1999), Ni/TiO_2 (Masai et al., 1988), Ni/CeO_2 (Asmi et al., 2003), Ni/Perovskite (Goldwasser et al., 2003), and $Ni/Ce-ZrO_2$ (Lee et al., 2003) modified catalyst. It is noted that these catalysts contain basic support or additive. It has been suggested that carbon deposition can be suppressed when nickel is deposited on the supports with strong Lewis basicity which can be achieved by addition of alkaline earth oxides to the support. Because carbon dioxide is well known as an acid gas, the increase in the Lewis basicity is expected to strengthen the ability of the catalyst to chemisorb carbon dioxide and reduce carbon formation via Boudouard reaction by shifting the equilibrium concentration. On the other hand, the addition of basic promoters can also lead to both catalyst stability and the enhancement of deposited carbon.

Moreover, using Ni catalyst on the other kinds of support, such as on the ceramic foam, which was a macro porous medium, was also investigated. According to the research of Takano et al. (1994,1996), the ceramics foam codiarite coat Al_2O_3 supports catalyst show high activity with a good stability and suppressed the increase of pressure drop in continuous flow reactor due to its high porosity.

The effect of Ni diameter was also investigated. It was indicated that the amount of carbon deposition based on the surface of Ni atom increased as the diameter of Ni increased. Therefore, it was presumed that catalyst with larger Ni diameter enhanced plugging more readily.

Furthermore, addition of a promoter to Ni catalyst has been reported that the rate of coke deposition was lower. Doping of some kinds of metal such as Sn (Hou et

al., 2004) or Ca (Hou et al., 2003) in a small amount in Ni/Al_2O_3 catalyst improved the dispersion and increased the reducibility of Ni catalyst and retarded the sintering of active Ni particle, which could improve the stability of the catalyst. Because the coke formation would require a bigger ensemble sites, the formation of surface intermetallic compound (such as Ni_3Sn) hindered the dissolution of carbon in Ni crystals while adding potassium metal in NiK/Al_2O_3 (Juan-Juan et al., 2004) promoted the reduction of Ni and hindered the coke deposition. This species gasified coke without any structural modification of nickel during reaction at 973 K. However, the surface enriched with these additives in excess amount, would hinder the access of CH_4 and/or CO_2 on the surface of Ni particles and depress its activity.

From early research on the effect of catalyst support, Uchijima et al. (1993), working with Rh/SiO_2, observed promotional effects for both the carbon dioxide reforming of methane and RWGS reactions when some Al_2O_3, TiO_2 or MgO was added to the catalyst. Moreover, Takano et al. (1994, 1996) investigated the reforming of methane with carbon dioxide using various Ni catalysts, including industrial stream reforming catalyst and industrial methanation catalyst. Among various supports, catalyst activity varied with the kind of support according to the following order; $Al_2O_3 > SiO_2$ with MgO $> SiO_2$ It was therefore argued that the promotional effect for carbon dioxide reforming could not be due to difference in metal distribution or the metal-support interaction.

It was interpreted in terms of carbon dioxide activation and the role of the mildly basic oxide in sufficiently improving the adsorption strength of carbon dioxide (in the form of carbonate or formate) for it to migrate to the active Rh and Ni sites. Al_2O_3 has basic nature, not like SiO_2. Addition of SiO_2 with MgO would increase the basicity of the support than only SiO_2 because of their base nature. This interpretation is in line with the mechanism suggested for carbon dioxide activation on alkali metal-containing platinum group metals (Solymosi et al., 1991), it is also documented that some oxide supports exert significant influence on the reactivity of carbon that forms on the surface of the catalytic metals (Solymosi et al., 1993).

3.2 Effects of operating parameters on carbon dioxide reforming of methane

Many researchers have been investigated to study the effects of many operating parameters on carbon dioxide reforming of methane over several kinds of supported catalysts, under various experimental variables such as temperature, CO_2/CH_4 feed ratio, and pressure.

Takano *et al.* (1994, 1996) reported that conversion of methane increases with increasing of reaction temperature. For $Ni/SiO_2,MgO$ catalyst, the pressure drop in reactor increased at temperature below 1000 K, did not change during the reaction temperature of 1030 K and decreased at higher temperature than 1060 K. This suggested that the rate of deposition and decomposition of carbonaceous deposits balanced at 1030 K.

Fraenkel et al. (1986) investigated the reforming reaction at the temperature range from 400-1000°C using a CO_2/CH_4 feed ratio of l/l at pressures of 1 and 10 atmospheres. They indicated that conversion of methane would be increased with higher reaction temperature. At 900°C the methane conversions are 97 and 90% at 1 and 10 atmospheres, respectively. The report also indicated that formation of water decreased with increasing temperature. The formation of water effectively disappears above about 900°C, due to less thermodynamically feasible at high reaction temperature.

The investigations were conducted by varying ratio of reactants CO_2/CH_4 from 0.5 to 5 over Ni/Al_2O_3 catalyst (Takano *et al.*, 1994, 1996) and from 0 to 1.6 over Pt/Al_2O_3 catalyst (Gustafson *et al.*, 1991). Conversion of methane increases with the increase of feed ratio of CO_2/CH_4. A lower CO_2/CH_4 ratio was preferred in order to increase the selectivity to H_2. The product CO/H_2 ratio proceeds towards unity as carbon dioxide in the feed is reduced, indicating that the hydrogen consumption resulted from RWGS reaction is increasingly restricted due to the unavailability of carbon dioxide. Nevertheless, increasing CO_2/CH_4 ratio would decrease carbonaceous deposition and pressure drop in the plug flow reactor.

Concerning the effect of operating pressure, Fraenkel *et al.* (1986) derived the thermodynamic equilibrium under two different pressures of 1 and 10 atmospheres. The carbon deposition threshold curves indicated that carbon deposition is thermodynamically possible for a CO_2/CH_4 reforming feed ratio of l/l at temperatures up to 1000°C at 1 atmosphere and 1100°C at 10 atmospheres. Moreover, at the same reaction condition, conversion of CH_4 would be reduced with increasing total pressure.

3.3 Combined carbon dioxide reforming and partial oxidation of methane

The reforming of methane with carbon dioxide and oxygen was first studied by Vernon *et al.* (1992). They reported that transition metals supported on inert oxides are active for this reaction. High yields of syngas were obtained without carbon deposition by using a 1%Ir/Al_2O_3 catalyst at 1050 K. They were also able to manipulate the CH_4:CO_2:O_2 ratio in order to achieve a thermo-neutral reaction.

Choudhary *et al.* (1995) have also studied this reaction over NiO/CaO and NiO/MgO catalyst, conversions above 95% were obtained and the catalyst did not deactivate during 20 hours on stream at 850°C. Ruckenstein *et al.* (1998) also found that NiO/MgO catalyst has high activity and selectivity, and the formation of a solid solution inhibits the carbon deposition.

Several nickel loaded catalysts, Ni/Al_2O_3, Co/Al_2O_3 and Fe/Al_2O_3 in combined carbon dioxide reforming and partial oxidation of methane have been reported by Tang *et al.* (1996). They found that Ni/Al_2O_3 is a better catalyst than Co/Al_2O_3 and Fe/Al_2O_3 as its yields of carbon monoxide and hydrogen are higher than the others. Moreover, nickel catalysts supported on different amounts of SrO modified SiO_2 was reported by Jing *et al.* (2004). They investigated under different temperatures, space velocities and feed gas composition. Results showed that the structure of nickel active phase is strongly dependent on the interaction between nickel and the support, which is related to the support properties, the additives and the

preparation methods. They found that SrO modified Ni/SiO$_2$ has a high and stable activity for this reaction, and presented stronger resistance to nickel aggregating, while the unmodified Ni/SiO$_2$ deactivated rapidly from nickel sintering. The enhanced interaction between nickel species and SrO promoted support might be responsible for its high activity and good resistance to agglomeration of the nickel particles.

From early research on Pt/ZrO$_2$ catalyst, Keulen *et al.* (1997) reported that it is an active catalyst for the carbon dioxide reforming of methane. However, some deactivation of the catalyst occurred during the first 300 hours of a 1000 hours test. Then, Aisling *et al.* (1998) used this catalyst in combined carbon dioxide reforming and partial oxidation of methane. They obtained higher yields of syngas at lower temperature than would be obtained with carbon dioxide reforming of methane alone. Furthermore, the loss of activity of the catalyst with time on stream decreased with the amount oxygen added to the feed stream, a small amount of carbon deposition occurred in parts of the catalyst bed which were not exposed to oxygen.

When Pt/ZrO$_2$ catalyst was compared to Pt/Al$_2$O$_3$ and Pt/10%ZrO$_2$/Al$_2$O$_3$ catalysts in temperature range of 450-900°C, it was found that Pt/10%ZrO$_2$/Al$_2$O$_3$ is the most active and stable catalyst for combined carbon dioxide reforming and partial oxidation of methane. They reported that the carbon deposition during this reaction is influenced by the supports. With small and highly dispersed particles over zirconia-alumina catalyst, the higher stability of the Pt/10%ZrO$_2$/Al$_2$O$_3$ catalyst is related to its coking resistance, which Pt-Zr^{n+} interacts at metal-support interface.

Additionally, the serious temperature gradient of catalyst bed in combined carbon dioxide reforming and partial oxidation of methane has been studied by Tomishige et al. (2002). They reported that Pt/Al$_2$O$_3$ is much flatter than Ni/Al$_2$O$_3$ catalyst. Then, Pt-Ni/Al$_2$O$_3$ catalyst prepared by the sequential impregnation method with small amount of Pt (0.45×10^{-5} mol/g.cat) exhibited very flat temperature profile in this reaction. Moreover, the effect of metal loading on Ni/Al$_2$O$_3$ and Pt/Al$_2$O$_3$ and Ni catalyst (G-91) on the temperature profile were investigated. Results showed that the temperature at catalyst bed inlet over Pt(10)/Al$_2$O$_3$ and Pt(1)/Al$_2$O$_3$ catalysts was much lower than that over Ni(10)/Al$_2$O$_3$, Ni(30)/Al$_2$O$_3$, G-91, Pt(0.3)/Al$_2$O$_3$. This

indicates that the combustion and reforming zones overlap in the case of $Pt(10)/Al_2O_3$ and $Pt(1)/Al_2O_3$ catalysts. But on other catalysts, the zones are separated. In terms of the energy efficiency in the syngas production by methane reforming, the overlap is very effective.

The addition of oxygen to carbon dioxide reforming of methane process has been studied by Connor *et al*. (1998) and also Pan *et al*. (2002). The results are in good agreement that the addition of oxygen to the feed stream increases methane conversion, especially at temperatures below 1100 K because methane is consumed in both carbon dioxide reforming and partial oxidation reactions. On the contrary, when the oxygen contents increases, the carbon dioxide conversion is decreased. However, as the combined carbon dioxide reforming and partial oxidation of methane process is basically a modified carbon dioxide reforming reactions, low temperatures and high oxygen contents are less in this process due to the significant loss in carbon dioxide conversion.

Reforming of methane with carbon dioxide and oxygen involves a coupling of methane oxidation with carbon dioxide reforming in the same reactor. Since, the rate of combustion is much higher than reforming. Therefore, a serious temperature gradient in the catalytic bed is occurred, leading to hot spots. Jing *et al*. (2004, 2005) studied this reaction over $Ni/MgO-SiO_2$ catalyst and found that a lot of whisker carbon was found on the catalyst in the rear of the fixed bed reactor, but no deposited carbon was observed in fluidized bed reactor after reaction. It leads to enhancement of methane and carbon dioxide conversion. This is suggested that fluidization of catalysts favors inhibiting deposited carbon and thermal uniformity in the reactor. The probable cause is that catalyst particles are circulated between the oxidizing and reducing zones and carbon gasification proceeds in the oxidizing zone.

3.4 Catalytic cracking of methane and catalyst regeneration reaction

The direct cracking of methane over supported nickel catalysts has recently been proposed as an alternative route for production of carbon monoxide free

hydrogen from natural gas ($CH_4 \leftrightarrow C + 2H_2$). Unlike other processes, which produce a mixture of hydrogen and carbon oxides, catalytic cracking produces hydrogen and solid carbon, eliminating the necessity for the separation of hydrogen from the other gaseous products.

The direct cracking of methane was early studied by Claridge et al. (1993). The rates of carbon deposition for the system with pure methane and pure carbon monoxide over a supported nickel catalyst at various temperatures were investigated. They showed that both Boudouard and methane decomposition are catalyzed depended on the operating temperature. At about 1050 K, the amount of carbon from pure carbon monoxide via the Boudouard reaction was very low compared with the amount from the methane decomposition reaction.

In order to enhance carbon production from CH_4 cracking, Ermakova et al. (2002) used Ni/SiO_2 catalysts prepared by heterophase sol-gel method with various stages of catalyst preparation. The carbon yield has depended only on the interaction between nickel and silica. The presence of silicates about 2 wt% in the 90% Ni–10% SiO_2 catalyst shows a rapid catalyst deactivation (the carbon yield is 40 g C/g Ni). The carbon yield as high as 384 g C/g Ni is observed with silicate-free 90% Ni–10% SiO_2 catalyst. It is assumed that silicate can either inhibit or promote formation of carbon depending on their amount comprised in Ni/SiO_2 catalysts.

When the catalyst deactivates due to carbon deposition, the catalyst regenerations by oxidation in air and steam gasification of deposited carbon have been proposed by Zhang et al. (1998). Both methods appear to be able to fully restore the activity of silica supported nickel catalyst in the catalytic cracking of methane at 823K. The XRD pattern suggests that the oxidation process completely removes the deposited carbon and converts the metallic nickel into nickel oxide, which needs to be reduced before next reaction cycle. On the contrary, the catalyst bed maintained the uniform temperature profile during the steam regeneration process and catalyst preserved its metallic nickel form at the end of process. Furthermore, the steam gasification leads to the production of the additional hydrogen with carbon monoxide

and methane as secondary products, formed due to the reverse water-gas shift ($CO_2+H_2 \leftrightarrow CO+H_2O$) and methanation ($CO+3H_2 \leftrightarrow CH_4+H_2O$) reactions.

3.5 Periodic operation

Periodic operation has been the subject of extensive experimental and theoretical investigations for three decades. Most of the studies on periodic operation reported in the literature have involved carbon monoxide oxidation and hydrogen production.

One of the first investigations of carbon monoxide oxidation under periodic operation was carried out by Cutlip (1979) who found that periodic switching between carbon monoxide and oxygen resulted in a significant increase in reaction rate. He ascribed this improvement to the shifting reactant coverage of the catalyst surface during periodic operation. Barshad et al. (1985) extended the study of carbon monoxide oxidation over Pd/γ-Al_2O_3 catalyst. They reported a 10-fold increase in carbon monoxide oxidation rate of a CO/O_2 ratio at 2393 K and split of 0.3 (based on the CO pulse), while of a CO/O_2 ratio at 1363 K and split of 0.3, greater than 15-fold increase was obtained.

For hydrogen production, the periodic operation of the catalytic cracking of methane reaction followed by the catalyst regeneration by burning of coke on modified Ni-gauze catalyst in oxidative oxygen atmosphere has been performed by Monnerat et al. (2001). The hydrogen production was studied as a function of the reaction temperatures and the variables of periodic operation like cycle period and cycle split. The optimal performance showed a maximum for a cycle period of 4 min and a cycle split of 0.5.

Another method for suppression of carbonaceous deposition is "D-R treatment". This pretreatment of catalyst was conducted on Ni/Al_2O_3 catalyst according to the paper of Ito et al. (1999), which is based on the hypothesis that active cores forming carbon whiskers are different from surface active sites for the main reaction on the catalyst. For this technique, one cycle consists of two steps. In the

deposition (D) step, methane was introduced to cause carbonaceous deposition and to grow carbon whiskers at 1000 K for 1 hour. The catalyst, which only participates in carbonaceous is detached from support. In the removal (R) step, carbon dioxde was introduced to remove carbon whiskers ($CO_2 + C \leftrightarrow 2CO$) at 1000 K for 1 hour. In this step, the growing cores with catalyst are removed and deactivated. The cycle is repeated several times.

The D-R treatment decreased the bulk nickel because a part of the nickel was removed from catalyst, which became the growing cores of carbon whiskers, and made catalyst inactive for carbonaceous deposition. This treatment accelerated the reforming activity, because the nickel located near the support was not influenced by the D-R treatment and the new sites for the reforming reaction were exposed by the removal of the bulk catalyst.

In the previous study of our group (Promaros et al., 2005) the performance of the periodic operation for the carbon dioxide reforming of methane over an industrial steam reforming $Ni/SiO_2 \cdot MgO$ catalyst compared with the steady-state operation at reaction temperatures 650 and $750^{\circ}C$ was investigated. It was found that methane conversions under periodic operation were lower than that of the steady state operation over all ranges of reaction time for both temperatures. At $750^{\circ}C$, the methane conversion and hydrogen yield initially decreased with time on stream giving the values about half of those from the steady state operation. The decreased catalytic activity was due to the accumulation of carbonaceous deposit and loss of metal active sites. The different trend was observed at 923 K. The methane conversion and hydrogen yield were not changed with time on stream although more carbonaceous deposit was accumulated during the reaction course. At this temperature, the periodic operation offered the equivalent hydrogen yield to the steady state operation. The observed behavior may be due to the different kinds of carbon formation over the catalyst. Further investigations are required to elucidate this unusual behavior.

Next study (Pholjaroen et al., 2006), the carbon formation taking place in the periodic operation of the carbon dioxide reforming of methane was investigated by using various analytical methods including BET surface area measurement, SEM,

XRD, and TPO in order to characterize the coke formed at various reaction times. It was found that at least two different cokes were formed on the surface of catalyst at this temperature range. At low temperature, coke was formed in a great amount in the methane cracking period but was incompletely removed in the regeneration period. At this temperature, coke was mostly formed in the structure of filamentous carbon. In contrast, at high temperature, a lesser amount of coke was obtained but it was formed in encapsulating form. Thus, it affected the activity of catalyst.

CHAPTER IV
EXPERIMENTAL

This chapter explains the details of catalyst, experimental procedures and analytical techniques used in the present work. It is divided into four sections. First, the details of catalyst, dilution material, and reactant gas are provided in Section 4.1. The next section describes the experimental system and apparatus used for testing the reforming reaction (Section 4.2). The experimental procedures were explained in Section 4.3. Finally, the characterization of spent catalysts by various techniques such as BET surface area, SEM, XRD, and TPO are provided in Section 4.4.

4.1 Chemicals and Materials

4.1.1 Catalyst

In this research, an industrial steam reforming $Ni/SiO_2.MgO$ catalyst (commercial grade) was employed for the combined carbon dioxide reforming and partial oxidation of methane. Its shape is a cylindrical with 3×3 millimeters. The specific properties of this catalyst are presented in Table 4.1.

Table 4.1 The specific properties of catalyst used in this study

Catalyst	$Ni/SiO_2.MgO$
Ni content	55 %w/w
Support/co-catalyst	SiO_2, MgO
Surface area [m^2/kg]	1.21×10^5
Ni Surface area [m^2/kg]	8.37×10^3
Ni diameter [nm]	44

4.1.2 Dilution material

A dilution material is used for mixing with catalyst before starting the reaction in order to reduce the pressure drop and temperature gradients along the catalyst bed. In this research, Silicon dioxide (SiO_2) supplied by Fluka was chosen as a dilution material. Their average size is 40-100 mesh. All experiments were performed at $Ni/SiO_2.MgO$ catalyst to silicon dioxide weight ratio of 0.3:1.

4.1.3 Reactant gases

The reactant gases used in this study are ultra high purity grade (99.999%) and high purity grade (99.99%) as shown in Table 4.2. They are supplied by Thai Industrial Gas Limited (TIG).

Table 4.2 Reaction gases used for the experiment

Gas	Grade	Supplier
Methane	Ultra high pure	TIG
Carbon dioxide	Ultra high pure	TIG
Oxygen	High pure	TIG
Hydrogen	Ultra high pure	TIG
Argon	Ultra high pure	TIG

4.2 Experimental system

The experimental system consists of a fixed bed reactor installed in an electrical furnace. The reaction temperature is controlled by temperature controller with thermocouple. The reactant gases passing through the reactor were controlled by Solenoid valve and multitimer. The effluent gas was analyzed by a gas chromatography (Shimadzu GC-8A). The diagram of a lab-scale gas phase for combined carbon dioxide reforming and partial oxidation of methane is exhibited schematically in Figure 4.1.

4.2.1 Reactor

The fixed bed reactor was made from quartz tube with an inside diameter of 11 millimeters. It was placed in the vertical direction with downward gas flow. Catalyst was placed over the quartz wool, which was packed at the middle of reactor for supporting the catalyst bed.

4.2.2 Automatic Temperature Controller

This unit consisted of a magnetic solid state relay switch connected to a variable voltage transformer and a temperature controller (Shinko, Japan) connected to a thermocouple. Reaction temperature was measured by thermocouple attached to the catalyst bed in the reactor. The temperature set point is adjustable in the range of $0\text{-}1,000^{\circ}C$ at the maximum voltage of 220 V.

4.2.3 Electrical Furnace

The furnace with 2 kW heating coil was connected with the automatic temperature controller to supply heat for the reactor. The reactor could be operated from room temperature up to $800^{\circ}C$ at the maximum voltage of 220 V.
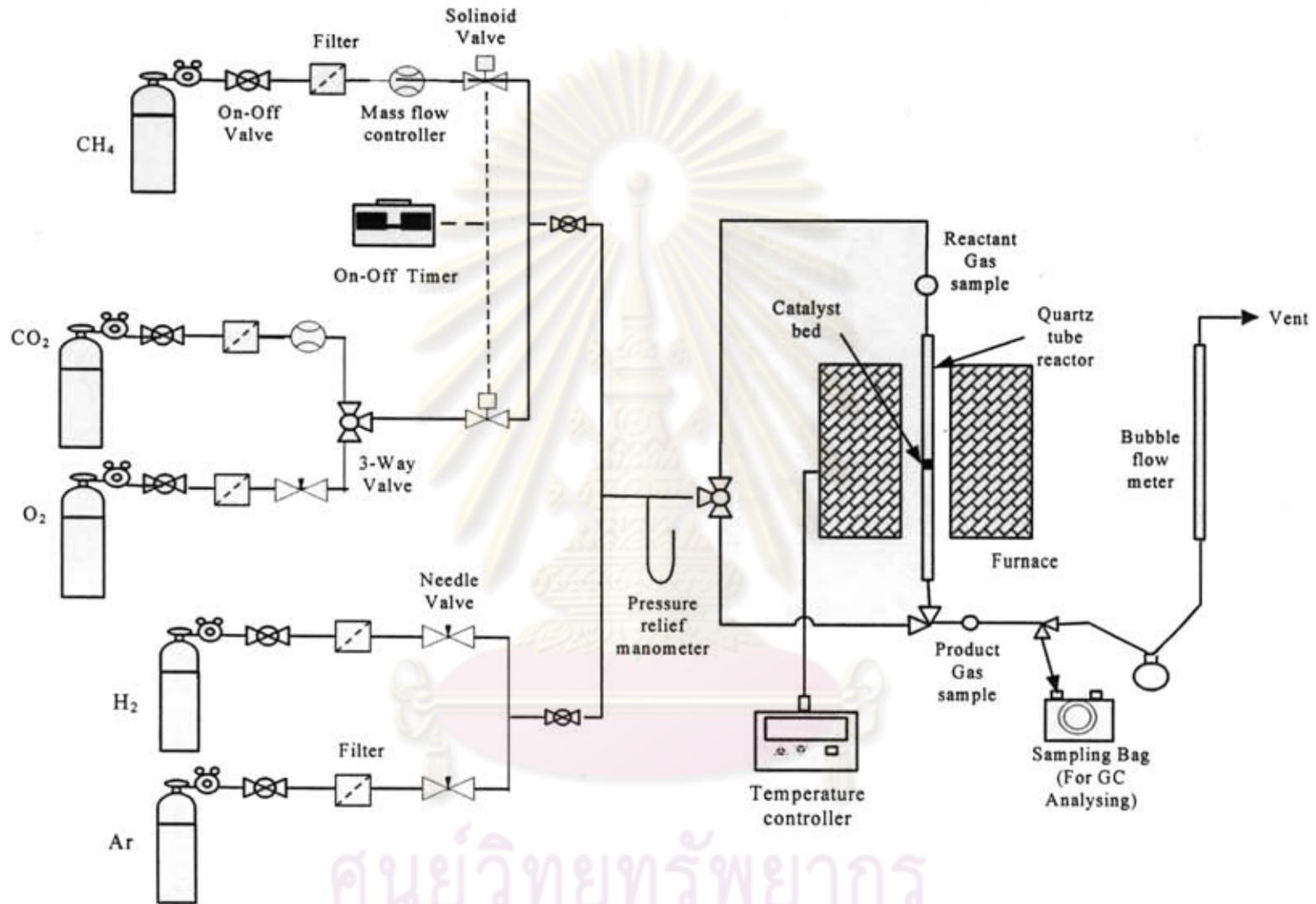
Figure 4.1 Schematic diagram of a lab-scale gas phase for combined carbon dioxide reforming and partial oxidation of methane

4.2.4 Gas Controlling System

Each reactant gas was equipped with a pressure gas regulator (0-120 psig) and an on-off valve. The flow rate was controlled by mass flow controller (GFC17S) operated under the flow range between 0-50 mL/min. For periodic operation, each reactant feed was switched between opening and closing periodically by using a solenoid valve (Flon industry, Japan) controlled by a multi-timer (Sibata BT-3).

4.2.5 Gas Chromatography

A gas chromatography Shimadzu modal 8A (GC-8A) equipped with a thermal conductivity detector (TCD) was used to analyze gas composition. Methane and oxygen in feed stream, carbon monoxide and hydrogen in the product stream was analyzed by using Molecular sieve 5A column. Carbon dioxide in the product stream was analyzed by using Poropak-Q column. The operating conditions for the gas chromatography are shown in Table 4.2.
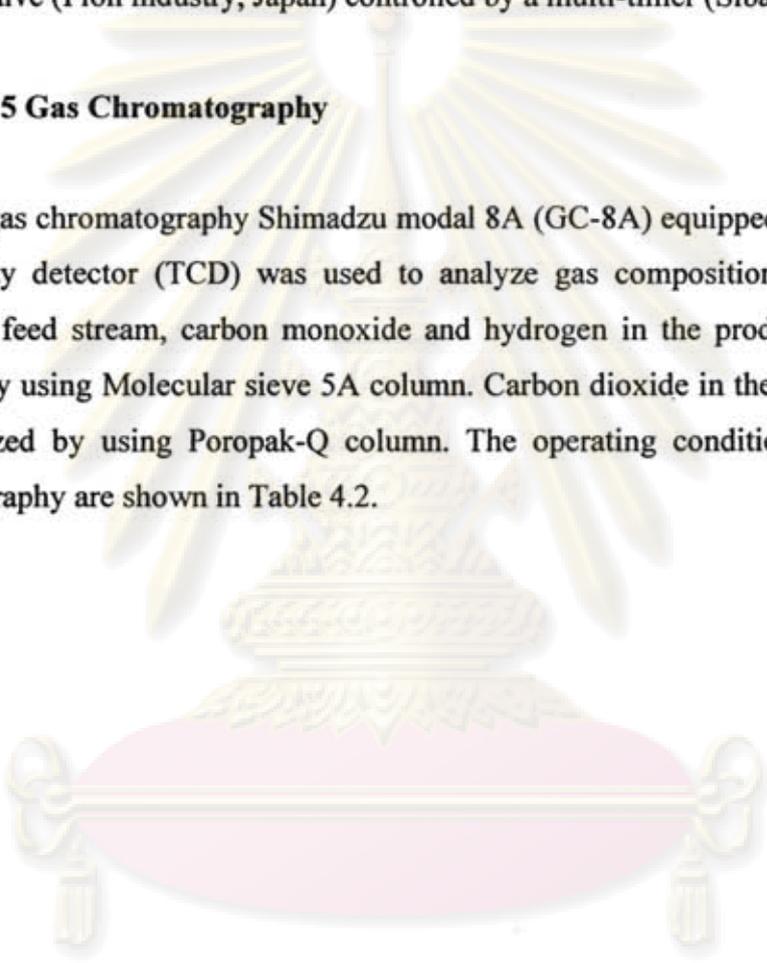
Table 4.3 Operating conditions for gas chromatograph

Gas Chromatograph	Shimadzu GC-8A	
Detector	TCD	
Column	Molecular sieve 5A	Porapak-Q
- Column material	SUS	SUS
- Length (m)	2	-
- Outer diameter (mm)	4	-
- Inner diameter (mm)	3	-
- Mesh range	60/80	-
- Maximum temperature ($^{\circ}$C)	350	-
Carrier gas	Ar (99.999%)	Ar (99.999%)
Carrier gas flow (ml/min)	30	30
Column temperature		
- initial ($^{\circ}$C)	70	70
- final ($^{\circ}$C)	70	70
Injector temperature ($^{\circ}$C)	100	100
Detector temperature ($^{\circ}$C)	100	100
Current (mA)	70	70
Analyzed gas	CH_4, H_2, CO	CO_2

4.3 Experimental procedures

For all experiments, the catalyst was prepared by mixing 0.1314 g of $Ni/SiO_2.MgO$ with 0.438 g of SiO_2. The mixture of catalyst was packed in the middle of the reactor and then placed in the electrical furnace. Before starting the reaction, the reduction of catalyst under hydrogen flow was conducted.

Reduction step:

The reactor was heated up to 650°C in argon flow of 30 mL/min. When the temperature reached to 650°C, the argon gas was switched off and the catalyst was reduced in hydrogen flow of 30 mL/min for 1 hour. After that, the system was purged in argon flow again for 10 minutes to remove hydrogen gas from the system.

Reaction step:

For steady state operation, the reaction was started by introducing CH_4, CO_2 and O_2 simultaneously to the reactor at reaction temperature of 650 and 750°C under total pressure of 1 atm. The molar flow rates of reactant gases are showed in Table 4.3. The gas sampling from product stream was taken every 20 minutes to analyze its composition by the TCD gas chromatography. The spent catalysts after exposed to the reactions for 200 minutes were characterized by various techniques including BET surface area, SEM, XRD, and TPO.

Table 4.4 The molar flow rates of reactant gases used for steady state operation

Reactants	Flow rate (mL/min)		
	$CH_4:CO_2:O_2=1:0.9:0.1$	$CH_4:CO_2:O_2=1:0.8:0.2$	$CH_4:CO_2:O_2=1:0.7:0.3$
CH_4	12.5	12.5	12.5
CO_2	11.25	10	8.75
O_2	1.25	2.5	3.75

For periodic operation, the multi-timer was set to control the solenoid valve to allow CH_4 pass through the reactor for 10 minutes in cracking step and then switch to combined CO_2 and O_2 for 10 minutes in regeneration step at various molar flow rates as showed in Table 4.4. However, between each cracking/regeneration step, the system was purged with argon for 10 min. The operation occurred repeatedly until the end of experiment. After completing each cracking/regeneration step, the product gas was collected by using a sampling bag. Then, its composition was analyzed by the TCD gas chromatograph. The spent catalysts after the reaction at 90, 100, 190 and 200 minutes were also characterized.

Table 4.5 The molar flow rates of reactant gases used for periodic operation

Reactants	Flow rate (mL/min)		
	$S_{CH4}=0.25$	$S_{CH4}=0.5$	$S_{CH4}=0.75$
CH_4	50	25	16.67
CO_2	15.08	22.5	45
O_2	1.6	2.5	5

Additionally, the effects of cycle period and cycle split on catalytic performance of reaction were investigated. All experiments were performed using CO_2/O_2 flow rate ratio of 9/1 at 650°C.

Effect of cycle period: The constant cycle split of 0.5 was conducted. Three values of cycle period of 10, 20 and 40 minutes were considered.

Effect of cycle split: The constant cycle period of 20 minutes was conducted. Three values of cycle split at 0.25, 0.5 and 0.75 were considered. The molar flow rates of the reactant gases at various cycle splits are showed in Table 4.5.

Table 4.6 The molar flow rates of reactant gases at various cycle splits

Reactants	Flow rate (mL/min)		
	S_{CH4}=0.25	S_{CH4}=0.5	S_{CH4}=0.75
CH_4	50	25	16.67
CO_2	15.08	22.5	45
O_2	1.6	2.5	5

4.4 Catalyst characterization

4.4.1 BET Surface Area Measurement

The total surface area, pore volume and pore size of catalysts were determined using a Micromeritrics model ASAP 2020. The sample cell which contained 0.3 g of sample was placed into Micromeritrics model ASAP 2020. After degassing step, N_2 physisorption was carried out for measuring the surface area and pore volume of catalyst.

4.4.2 X-ray diffraction (XRD)

The crystallinity and X-ray diffraction patterns of the fresh and spent catalysts were performed by an X-ray diffractometer, SIEMENS D5000, using Cu Kα radiation with Ni filter. The operating conditions of measurement are shown follows:

2θ range of detection: 10-80°

Resolution: 0.04°

Number of scan: 20

4.4.3 Scanning electron microscopy (SEM)

Scanning electron microscopy (SEM) was used to determine the catalyst granule morphology, using a JEOL JSM-35CF scanning electron microscope. The SEM was operated using the back scattering electron (BSE) mode at 15 kV at

Scientific and Technological Reseach Equipment Centre, Chulalongkorn University (STREC).

4.4.4 Temperature-Programmed Oxidation (TPO)

Temperature-programmed oxidation was used to characterize the coke deposited on the catalysts. The operation was performed by using Micromeritrics Chemisorb 2750. Most amount of sample after the reaction was pre-treated in He (25 mL/min) at 250°C for 1 hour for eliminating moisture from the catalyst and cooled down to room temperature. Then 1 vol% oxygen in helium (15 mL/min) was switched into the sample while the system was heated at 10°C/min to 1000°C and the exit gas was detected by a TCD detector. The calculation of amount of CO_2 in the effluent gas was analyzed and reported by Chemisorp TPx software.
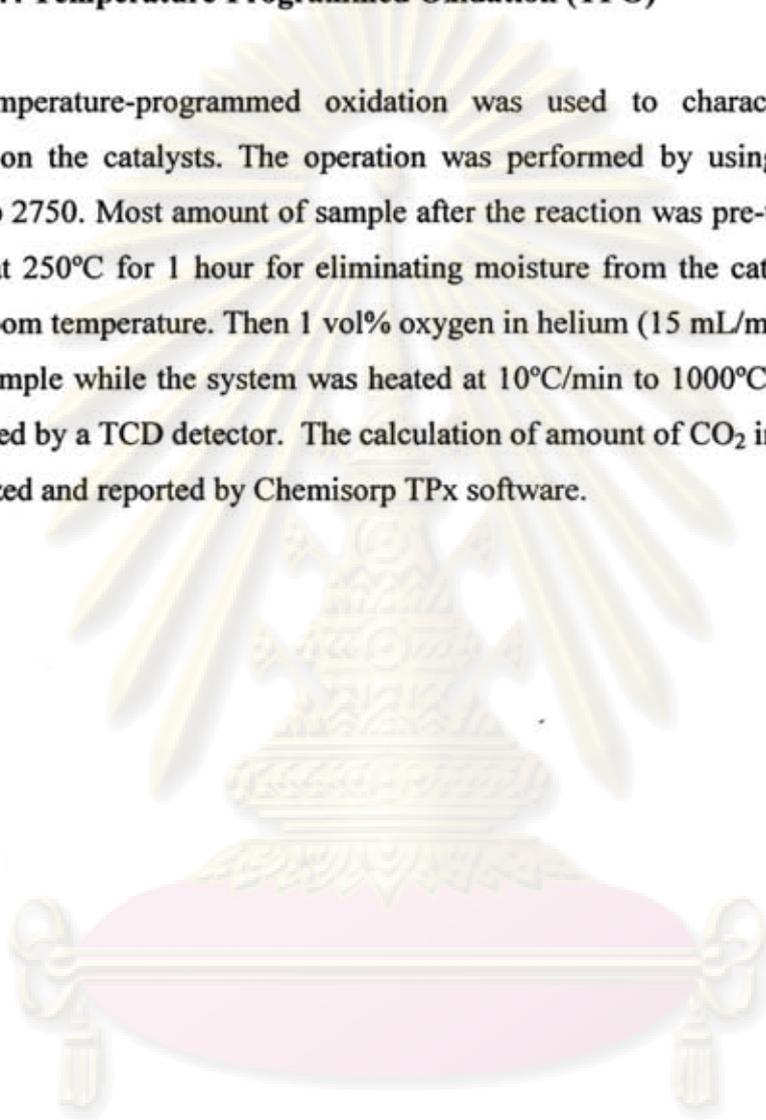
CHAPTER V
RESULTS AND DISCUSSION

This work investigated the catalytic performance of combined carbon dioxide reforming and partial oxidation of methane over industrial steam reforming $Ni/SiO_2.MgO$ catalyst under both periodic and steady state operations. The results and discussions in this chapter are divided into three main parts. In the first part, the effects of oxygen addition and the reaction temperatures on the catalytic activity of the reaction were investigated. The second part describes the characterization of the catalysts after the reaction at various reaction times and temperatures. The degrees of coke formation at different oxygen contents under periodic operation were also discussed and compared with those from steady state operation. In the last part, their performances at different cycle periods and cycle splits under periodic operation were determined and also compared with those from steady state operation.

## 5.1 Catalytic Activity in Combined Carbon Dioxide Reforming and Partial Oxidation of Methane

This part focused on the effect of oxygen addition and reaction temperatures. The methane flow rate was set constant while the CO_2/O_2 flow rate ratios (10/0, 9/1, 8/2, 7/3) and the reaction temperatures ($650^{\circ}C$, $750^{\circ}C$) were varied under both periodic and steady state operations. For periodic operation, the reaction was started by feeding the reactants alternately between methane in the cracking step ($CH_4 \rightarrow C + H_2$) and combined carbon dioxide with oxygen in the regeneration step ($C + CO_2 \leftrightarrow 2CO$, $C + 1/2O_2 \rightarrow CO$, $CO + 1/2O_2 \rightarrow CO_2$). For steady state operation, the reaction was carried out by feeding methane, carbon dioxide and oxygen simultaneously. It should be noted that the average total flow rates of feeds for both operations were identical. The catalytic activities in term of methane conversion, carbon dioxide conversion, and hydrogen yield for both operations with different oxygen addition contents and reaction temperatures were investigated. The results of activities under periodic operation were shown in Figures 5.1-5.4 whereas those under steady state operation were shown in Figures 5.5-5.10.
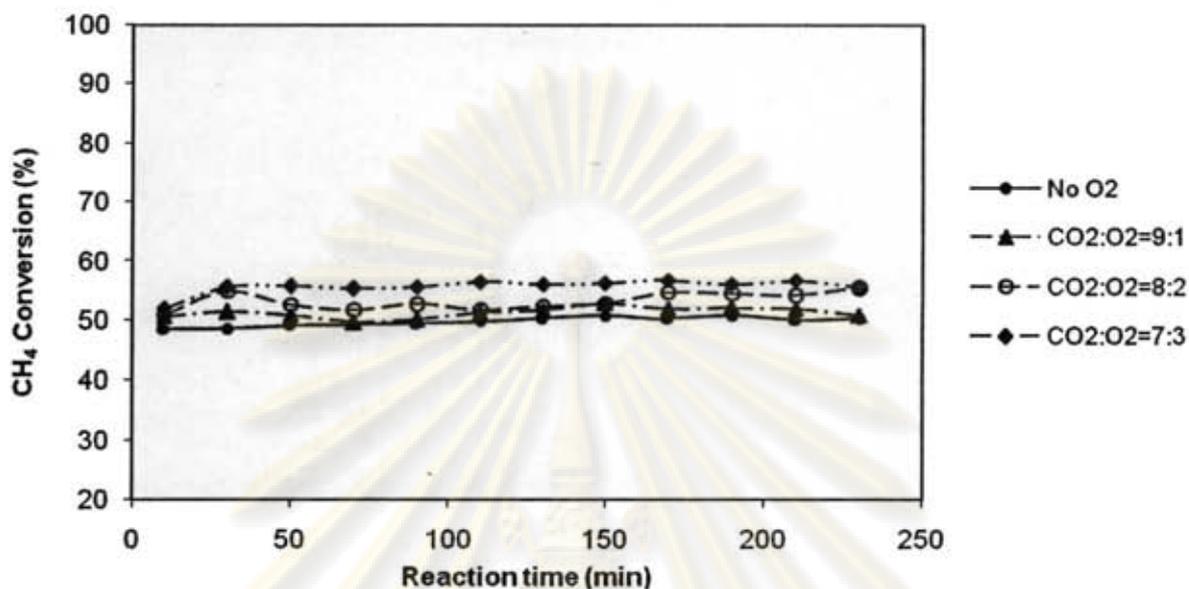
Figure 5.1 Methane conversions in combined carbon dioxide reforming and partial oxidation of methane under periodic operation at 650 °C with different oxygen contents.
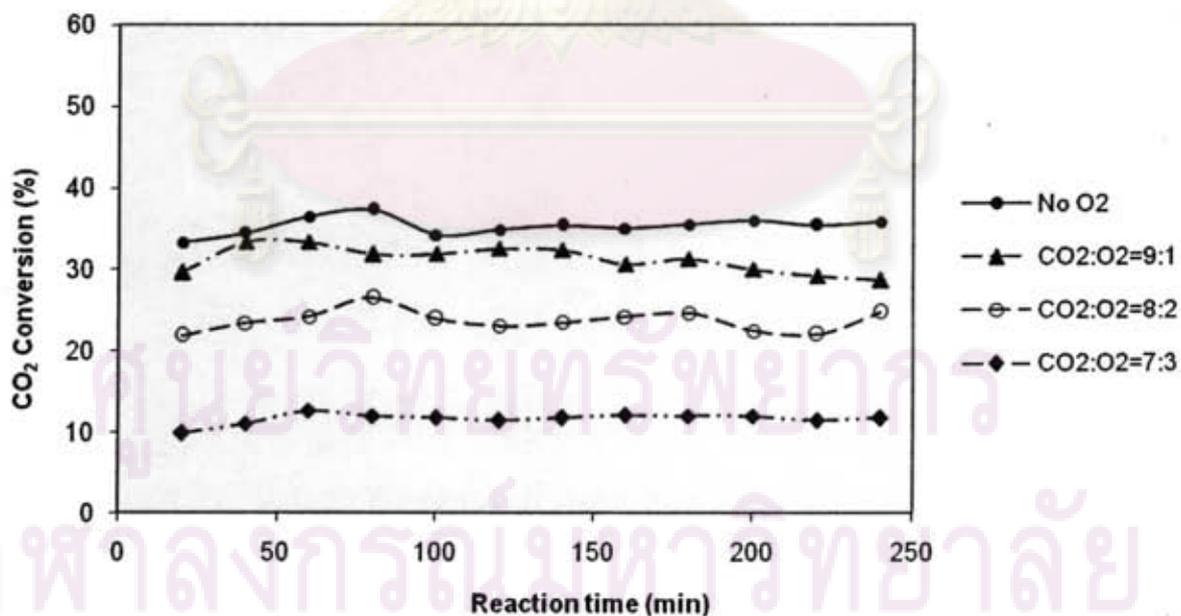
Figure 5.2 Carbon dioxide conversions in combined carbon dioxide reforming and partial oxidation of methane under periodic operation at 650 °C with different oxygen contents.
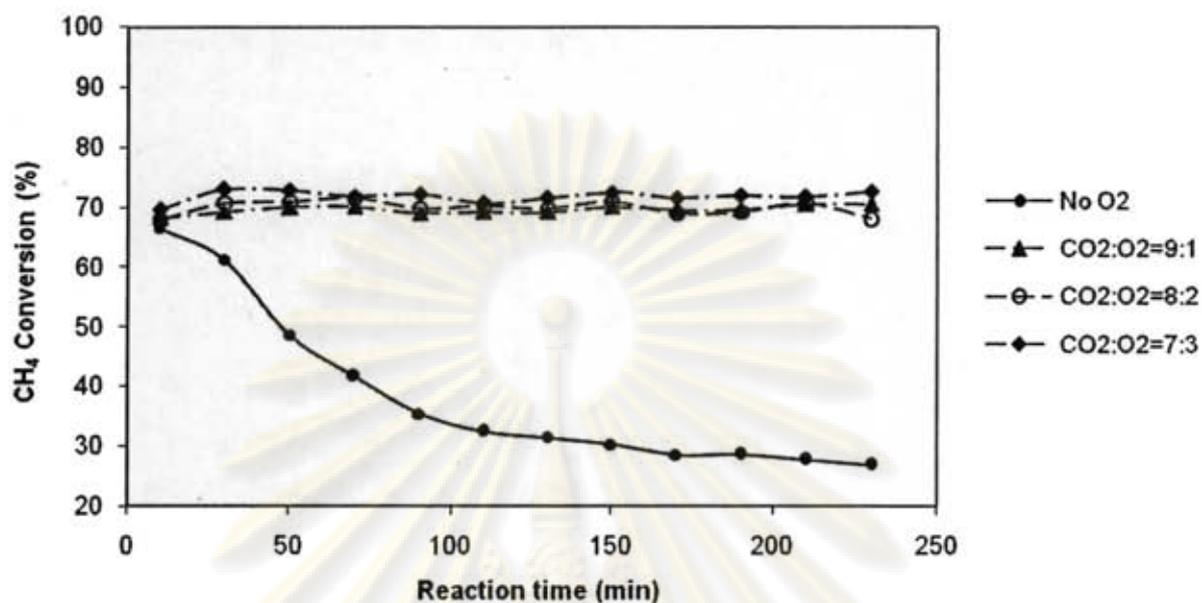
Figure 5.3 Methane conversions in combined carbon dioxide reforming and partial oxidation of methane under periodic operation at 750 °C with different oxygen contents.
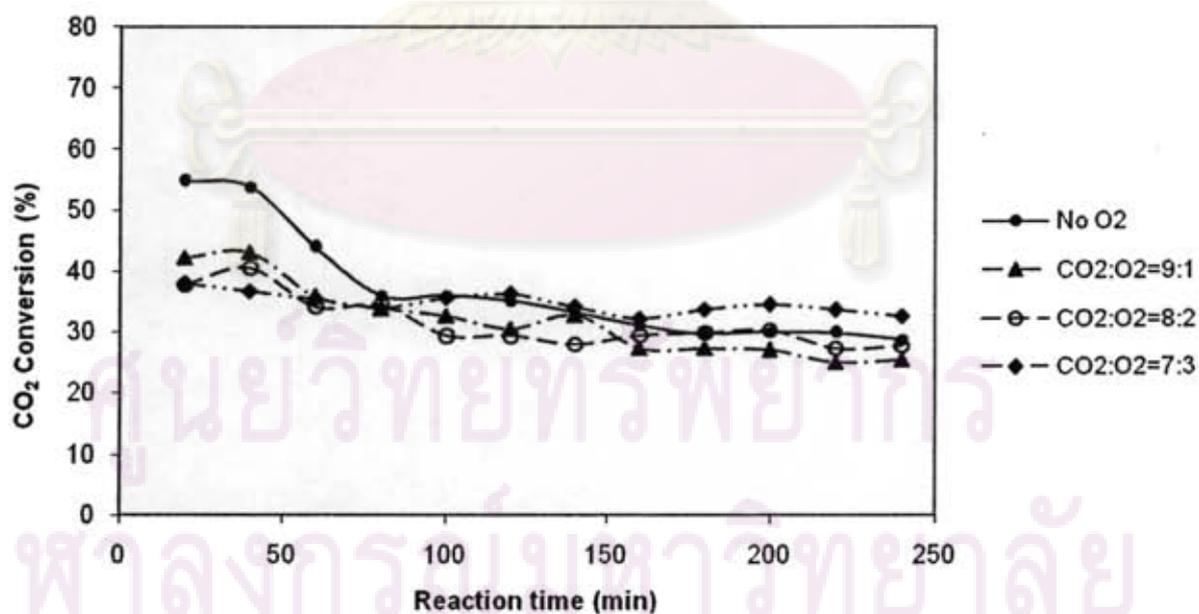
Figure 5.4 Carbon dioxide conversions in combined carbon dioxide reforming and partial oxidation of methane under periodic operation at 750 °C with different oxygen contents.
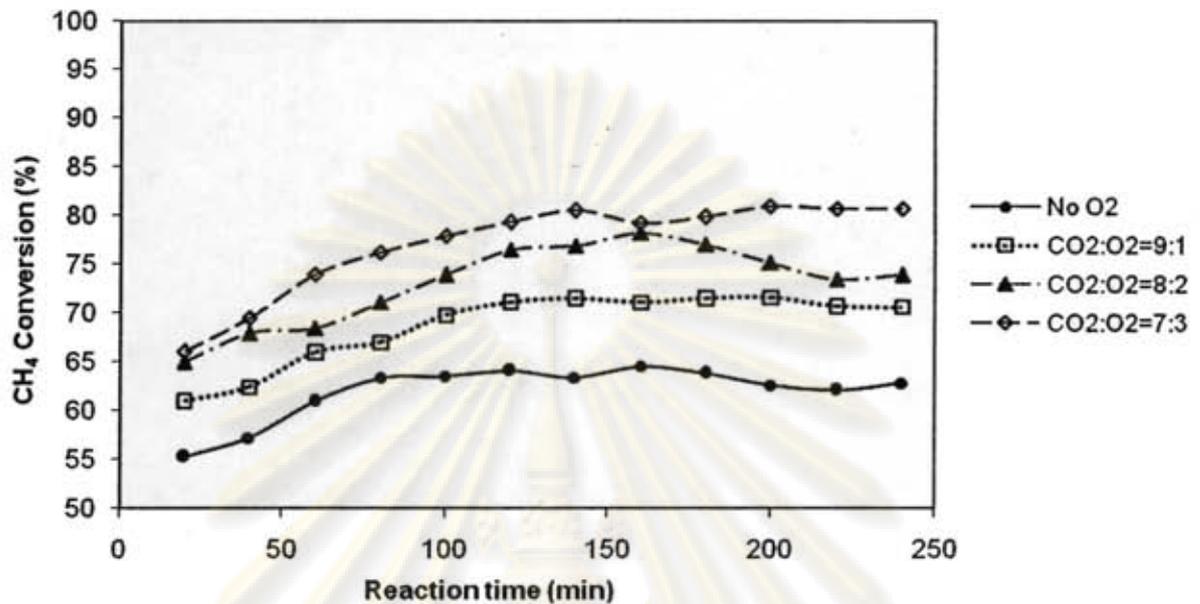
Figure 5.5 Methane conversions in combined carbon dioxide reforming and partial oxidation of methane under steady state operation at 650 °C with different oxygen contents.
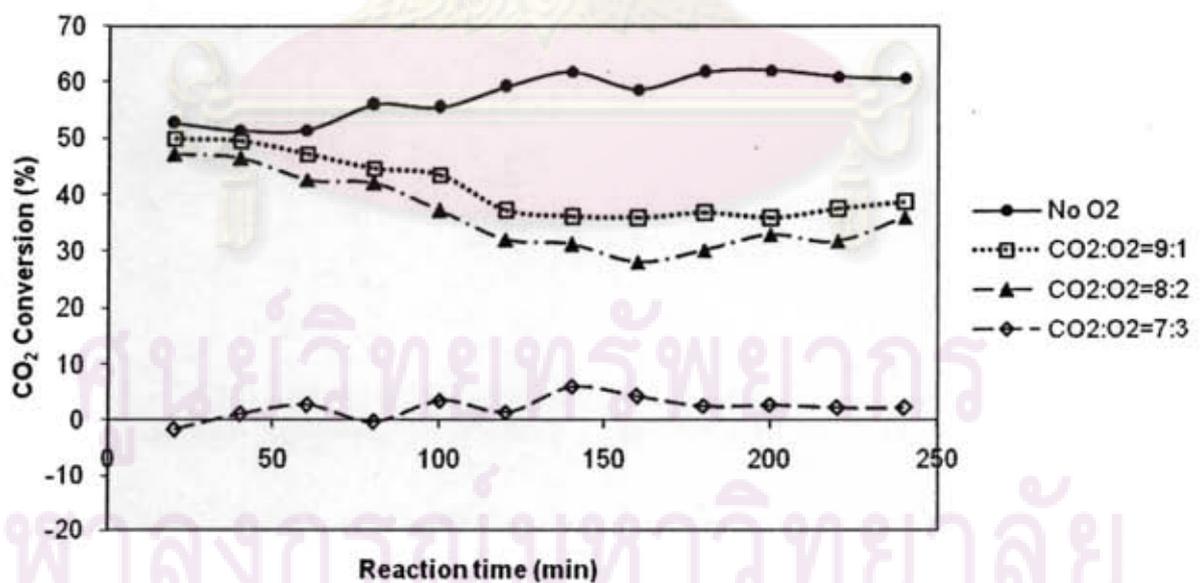
Figure 5.6 Carbon dioxide conversions in combined carbon dioxide reforming and partial oxidation of methane under steady state operation at 650 °C with different oxygen contents.
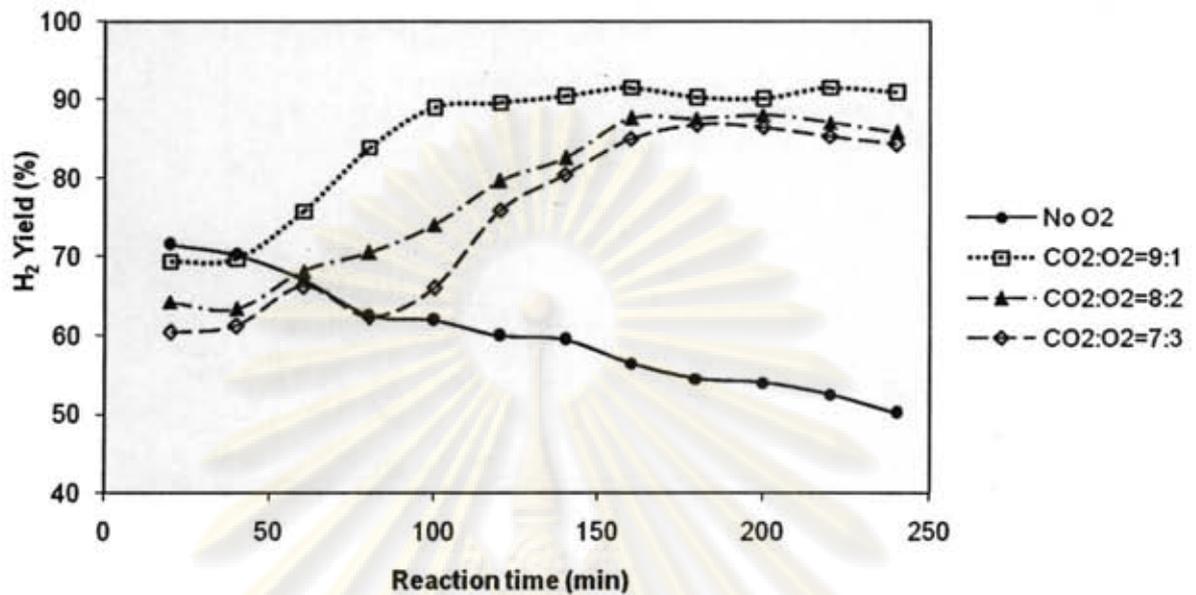
Figure 5.7 Hydrogen yields in combined carbon dioxide reforming and partial oxidation of methane under steady state operation at 650 °C with different oxygen contents.
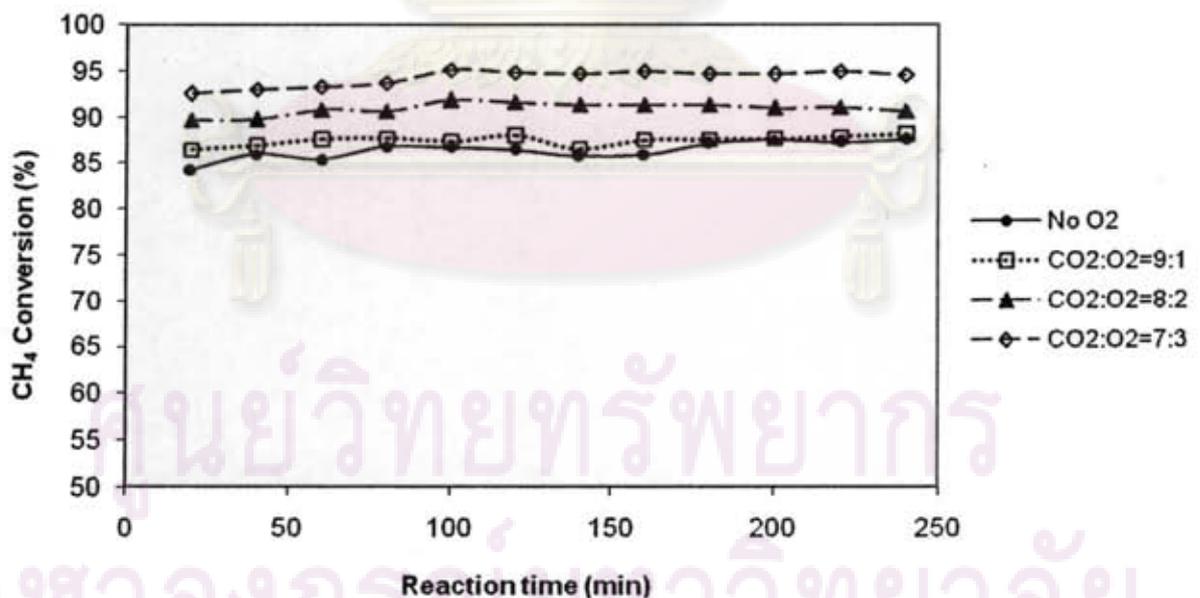
Figure 5.8 Methane conversions in combined carbon dioxide reforming and partial oxidation of methane under steady state operation at 750 °C with different oxygen contents.
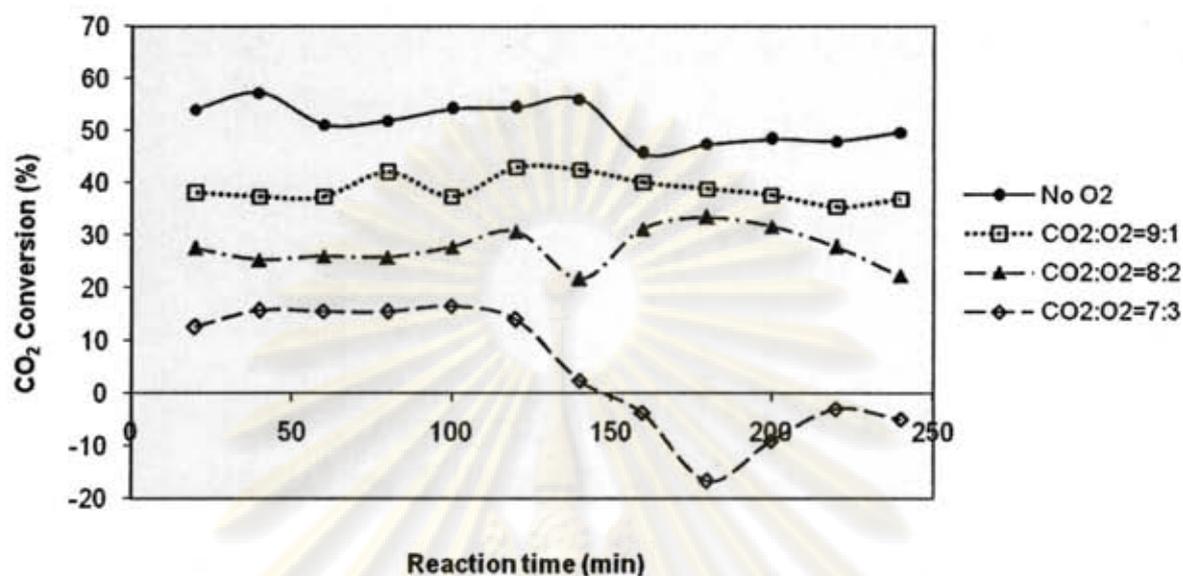
**Figure 5.9** Carbon dioxide conversions in combined carbon dioxide reforming and partial oxidation of methane under steady state operation at 750 °C with different oxygen addition contents.
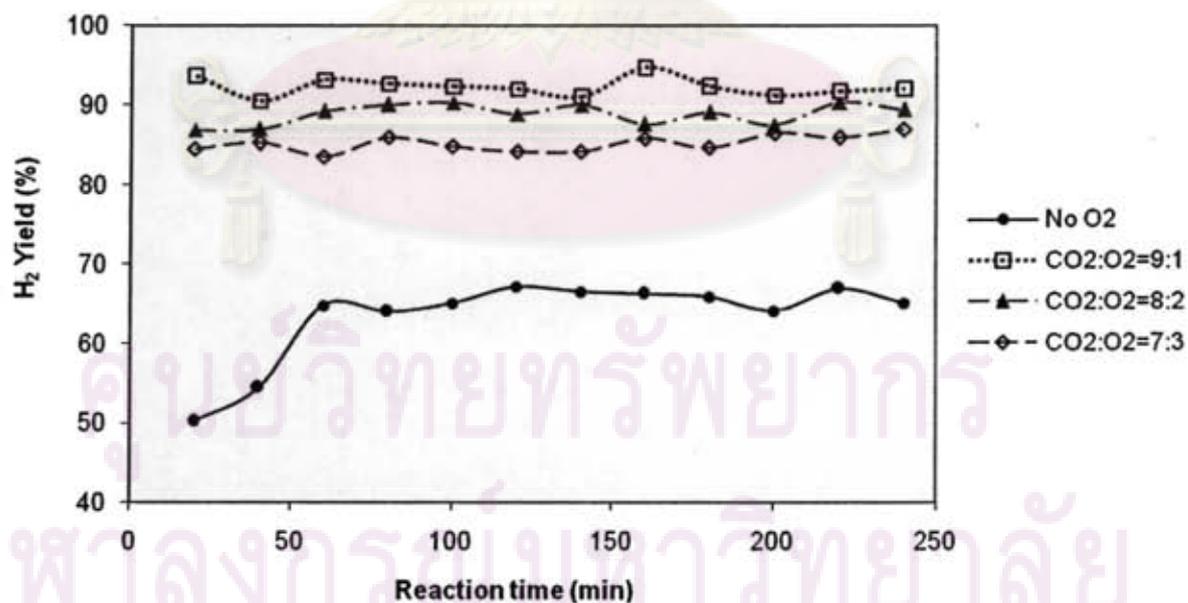

Figure 5.10 Hydrogen yields in combined carbon dioxide reforming and partial oxidation of methane under steady state operation at 750 °C with different oxygen contents.

The results show that when the different oxygen contents were introduced into the reactor under periodic and steady state operations at various temperatures, there was a noteworthy effect on both methane and carbon dioxide conversions. Since oxygen is an active species, the oxygen conversion about 100% was obtained for both operations as observed in this study.

Under periodic operation, the oxygen addition increased methane conversion from about 49% to the maximum value of about 56% at low temperature (650°C). Especially at high temperature (750°C), it was able to improve the catalytic stability and obtain a higher value of methane conversion of about 72%. This is because the oxygen addition acted as a co-oxidant of carbon dioxide to accelerate the coke removal in the regeneration step without any deactivation of reforming activity. However, the effect of oxygen content was less significant on change of methane conversion at high temperature.

On the contrary, the carbon dioxide conversion decreased with increasing the oxygen content from about 35% to the minimum value of about 12% at 650°C and from about 29% to the minimum value of about 25% at 750°C as shown in Figures 5.2 and 5.4 respectively. Because the carbon dioxide conversion is one of the important targets, the high reaction temperature was more favorable for obtaining higher methane and carbon dioxide conversions. For hydrogen yield, the selectivity of methane to hydrogen production is considered to be equal to 100%. Thus hydrogen yield is equals to the methane conversion in this operation.

Under steady operation, the methane conversion tended to increase with increasing oxygen content and reaction temperature from about 62% to over 70% at low temperature and from about 85% to over 88% at high temperature as shown in Figures 5.5 and 5.8. This is because methane is consumed in both carbon dioxide reforming and partial oxidation reactions. But at the same time, the oxygen addition reduced carbon dioxide conversion from about 60% to below 38% at low temperature and from about 47% to below 36% at high temperature as shown in Figures 5.6 and 5.9. This is probably because oxygen reacted more easily with methane than carbon dioxide, resulting in lower carbon dioxide conversion. Moreover, this is probably affected by the occurrence the reverse water-gas shift reaction

(Eq.5.1). Therefore, the amount of carbon dioxide increases in product and the conversion drastically decreases.

$$CO_2 + H_2 \leftrightarrow CO + H_2O \qquad (5.1)$$

The oxygen addition also improved the hydrogen yield from about 50% to the maximum value of about 90% at low temperature and from about 65% to the maximum value about 91% at high temperature as shown in Figures 5.7-5.10. However, more oxygen content in the reaction caused slight decrease in hydrogen yield for both reaction temperatures. This is affected by the occurrence of the complete combustion of methane (Eq.5.2) which results in the reduction of hydrogen yield. In addition hydrogen product can directly react with oxygen to water (Eq.5.3)

$$CH_4 + 2O_2 \leftrightarrow CO_2 + H_2O \qquad (5.2)$$
$$2H_2 + O_2 \leftrightarrow 2H_2O \qquad (5.3)$$

Comparison between periodic and steady state operations for combined carbon dioxide reforming and partial oxidation of methane at reaction temperature of 650 and 750°C revealed that the periodic operation showed lower performance in term of methane conversion than those from the steady state operation at both temperatures. However, considering the obtained hydrogen yield, it was found that the periodic operation offered the hydrogen yield close to that of the steady state operation at 650°C. In the addition, the periodic operation also provides another benefit on the separated product streams of hydrogen and carbon monoxide. In order to investigate the accumulated coke on catalyst bed, the used catalysts after exposure in the reaction with different oxygen contents in each cracking/regeneration cycle under periodic operation were characterized and compared with those from steady state operation. The details are mentioned in the next part.

5.2 Characterization of Spent Catalysts

This part studied characteristics of spent catalysts by emphasizing on coke deposited on the catalyst surface under both periodic and steady state operations. All spent catalysts were exposed to the reactions at total reaction time of 200 minutes. The CO_2/O_2 flow rate ratios and reaction temperatures were varied at 10/0, 9/1, 7/3 and 650°C, 750°C respectively. Under periodic operation, the experiments were performed using a constant cycle time (τ) of 20 minutes and cycle split (s) of 0.5. Thus, reactants were feed alternately between methane and combined carbon dioxide with oxygen every 10 minutes. Four values of reaction times at 90, 100, 190, and 200 minutes were considered. The reaction times of 90 and 190 minutes stand for the used catalyst after cracking step at cycle number of 5 and 10 respectively, whereas the reaction times of 100 and 200 minutes stand for the used catalyst after regeneration step at cycle number of 5 and 10 respectively. For steady state operation, a mixture of methane, carbon dioxide and oxygen was fed simultaneously and reaction time of 200 minutes was considered. In order to understand the behavior of coke formation on surface of catalyst, various techniques were applied including BET surface area measurement, SEM, XRD and TPO.

Figure 5.11 shows the effects of oxygen content and reaction temperature on the changes in catalyst weight at various reaction times. After the catalyst was reduced with hydrogen to form an active metallic phase for the reforming reaction, the periodic operation was started. During the cracking step, the increase in catalyst weight by the coke formation on the catalyst surface was observed. While during the regeneration step, deposited coke was removed and its weight decreased. However, the change in catalyst weight was decreased with increasing the number of cycle.

The results show that lower amount of coke was formed in the system at higher reaction temperature and oxygen content. The similar tendency was found under the steady state operation as shown in Figure 5.12. These agree with those from the catalytic activity in previous part, i.e., their performances increased with increasing oxygen content and reaction temperature.
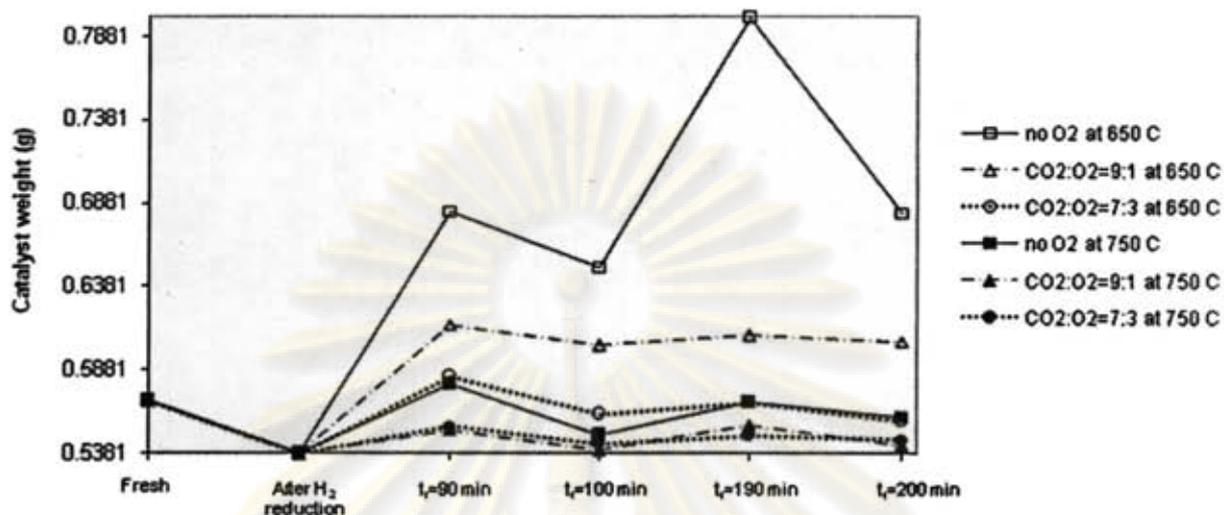
Figure 5.11 The effects of oxygen content and reaction temperature on change in catalyst weight at various reaction times
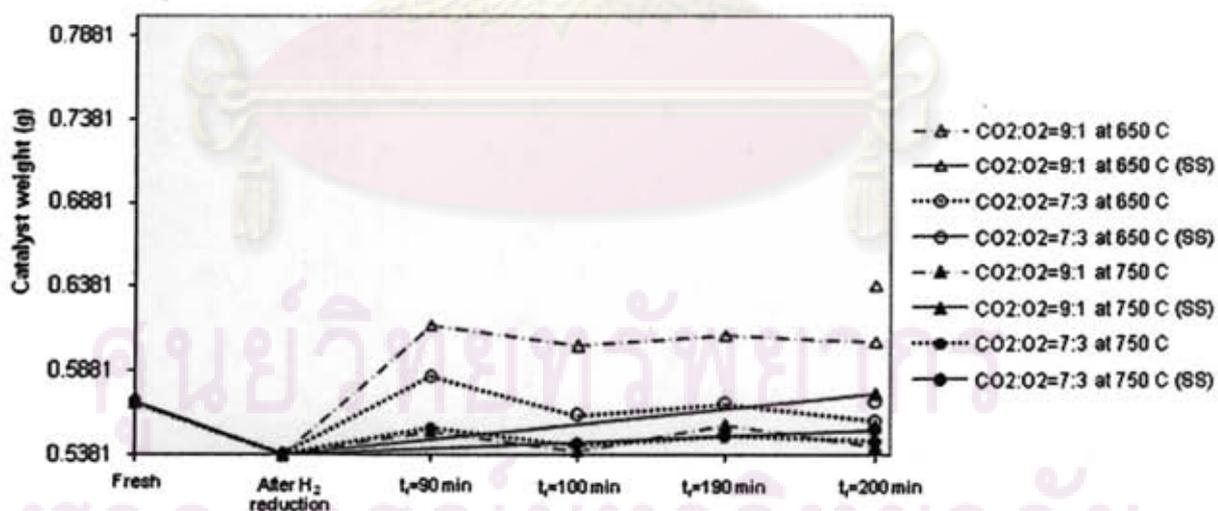
Figure 5.12 Comparison of change in catalyst weight between periodic and steady state operation with different oxygen contents and reaction temperatures at various reaction times

The BET surface area measurements of spent catalyst are summarized in Table 5.1. These results were corresponding to the results of catalyst weight; BET surface area increased during cracking step due to coke formation but decreased by coke oxidizing during regeneration step. At higher temperature, the lower of BET surface area was observed indicating that accumulated coke is lessened because filamentous carbon can be removed easily at high temperature (Takano et al., 1995). This result is in good agreement with previous study by Pholjaroen et al., (2007) that there are 2 types of coke forming on the surface of catalyst at different temperatures. At low temperature, coke mostly formed in filamentous carbon that appears the growing length with higher surface area and accelerates the rate of carbon deposition. Whereas at high temperature, a lesser amount of coke was obtained in encapsulating carbon that covers the catalyst surface and can block active sites of reforming reaction, the lower surface area was achieved. However, in this study the addition of oxygen which is an active oxidizing agent can improve the stability of the reaction by accelerating coke removal.

BET surface area of the spent catalyst was found to be lower than that of the reduced catalyst. Ito et al. (1998) explained that when the filamentous carbons having nickel cores on the growing top were oxidized during the regeneration step, the nickel cores fell on the surface and became inactive particles. Coalesce of inactive nickel cores on the bulk nickel surface to the larger size especially at high temperature caused the BET surface area to be decreased. Additionally, inactive nickel cores can suppress the active site for coke deposition without participation of active site for reforming reaction.

The oxygen addition into the regeneration step also affected to the BET surface area of catalyst. It was found that at higher oxygen content, lower surface area was obtained due to lower coke formation. Additionally, the BET study of spent catalysts under steady state operation at different conditions is also measured for comparison. The results show similar trend as periodic operation.

**Table 5.1** BET surface areas of catalysts at different conditions

Catalysts	Surface area (m^2/g)
Fresh	104.62
After reduction with H_2 at 650 °C 1 hr	46.96
After calcination in air at 750°C 3 hr	34.71
After calcination and reduction with H_2 at 750°C 1 hr	20.36

| Rxn.Temp.	Oxidant ratio	Operation	Reaction time			
			90 min	100 min	190 min	200 min
650°C	no O_2	Periodic	66.9	60.51	76.56	65.69
	$CO_2:O_2 = 9:1$	Steady state	-	-	-	42.41
		Periodic	52.74	25.21	81.88	33.94
	$CO_2:O_2 = 7:3$	Steady state	-	-	-	16.45
		Periodic	31.8	27.1	47.2	14.54
750°C	no O_2	Periodic	20.74	19.36	20.42	14.06
	$CO_2:O_2 = 9:1$	Steady state	-	-	-	35.95
		Periodic	10.14	5.34	22.25	6.38
	$CO_2:O_2 = 7:3$	Steady state	-	-	-	16.26
		Periodic	11.8	4.46	14.06	3.45

Scanning electron microscopy (SEM) technique was used to observe the catalyst samples that were conducted under periodic operation at CO_2/O_2 flow rate ratios 9/1 and 7/3 and reaction temperatures 650 and 750°C (Figures 13-14). All samples were tested after exposure in the reaction for 190 minutes, which was the ending time of methane cracking period. At low temperature, deposited coke presented in filamentous carbon structure on the surface of catalyst. Contrary at high temperature, no visible filamentous carbon was observed. It was also found that when the higher oxygen content was employed, the lesser amount of coke was observed.
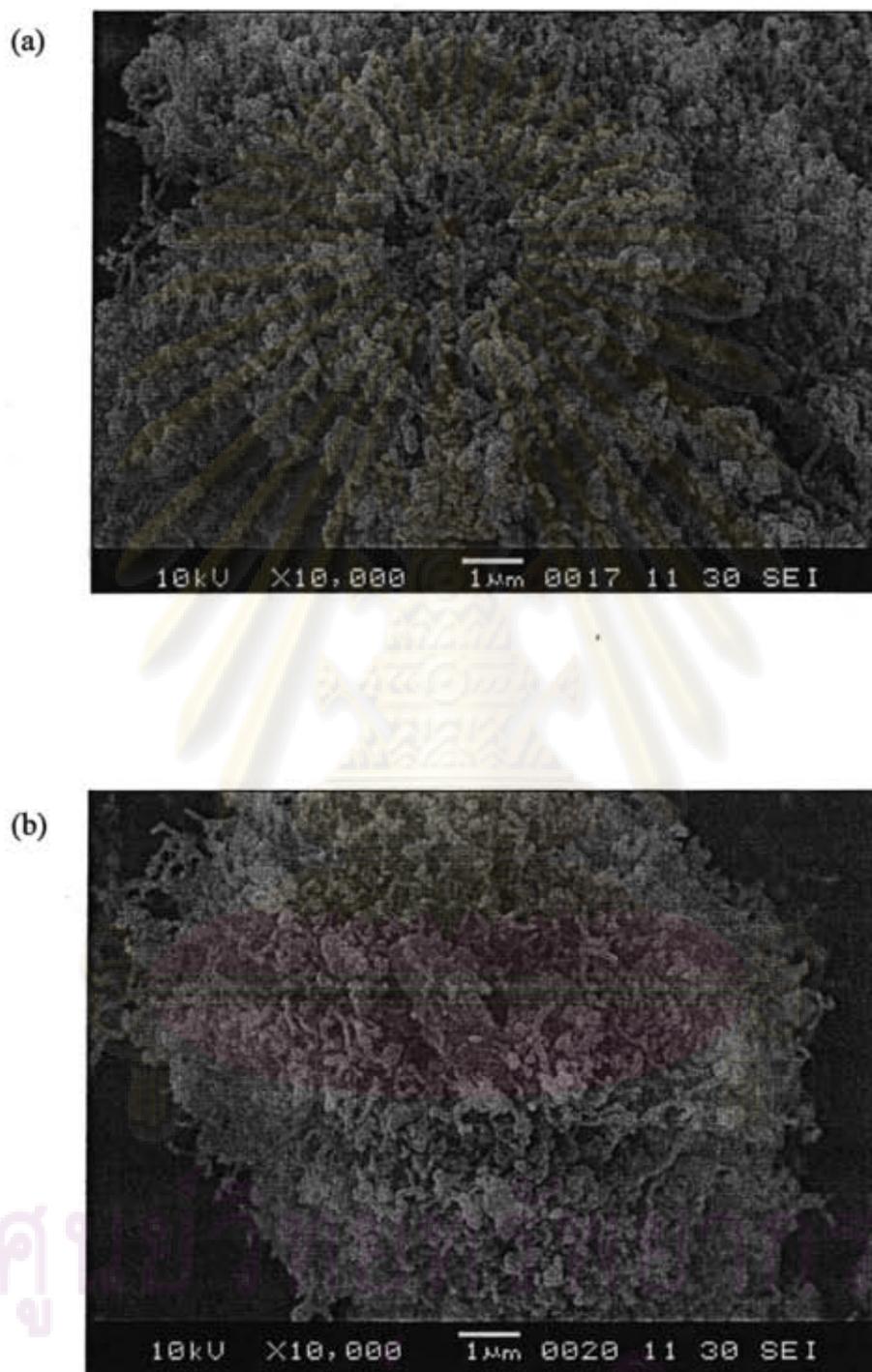
Figure 5.13 SEM micrographs of spent catalysts after exposure in the reaction for 190 minutes at 650°C with different reactant ratios   (a) $CO_2:O_2=9:1$ (b) $CO_2:O_2=7:3$
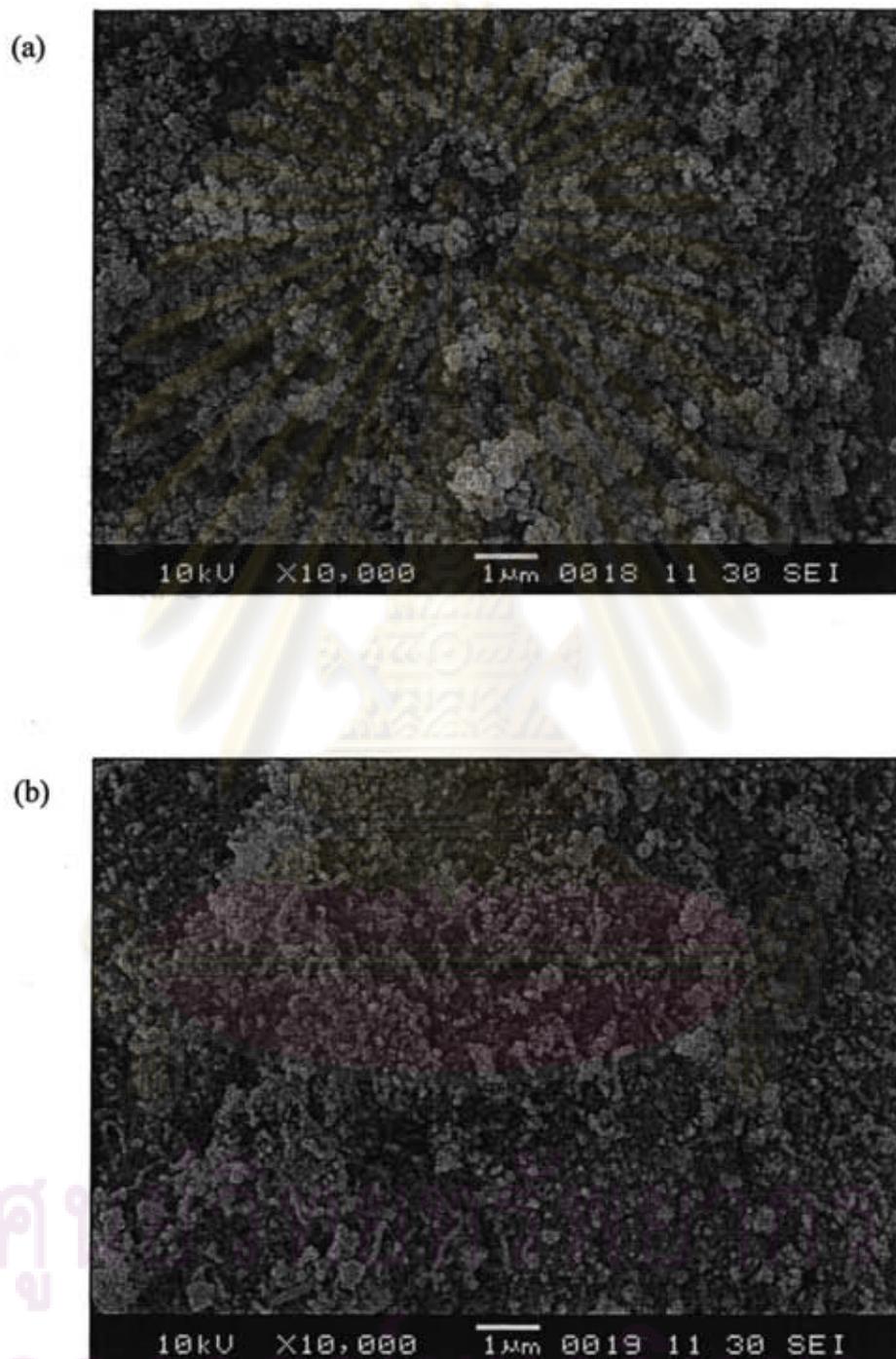
Figure 5.14 SEM micrographs of spent catalysts after exposure in the reaction for 190 minutes at 750°C with different reactant ratios   (a) $CO_2:O_2=9:1$ (b) $CO_2:O_2=7:3$

Spent catalysts were further studied by X-Ray diffraction (XRD). This technique was chosen to identify the crystal structure of Ni metallic and other metal forms on the catalysts. The characterizations were performed for the spent catalysts after the cracking and regeneration step under periodic operation at different oxygen contents and reaction temperatures. The measurement of the spent catalysts under steady state operation was also carried out for comparison as shown in Figures 5.15-5.16.

The XRD pattern of fresh catalyst indicated that nickel has crystal structure of NiO (peaks at $2\theta = 37.1, 43.1$ and 62.7) which would be reduced with hydrogen to convert nickel oxide into the metallic nickel before starting the reaction. It also indicated the presence of carbon of graphitic nature evident from the strong peak at $2\theta = 26.6°$ contaminated in the fresh catalyst sample as well as carbon accumulated in the spent catalysts. Under periodic operation, it was found that the presence of accumulated coke of graphitic nature on the catalyst surface was evident during the cracking step. After regeneration step, the intensity of this peak was considerably lower indicating that much of carbon was removed from surface of catalyst. While the metallic Ni peaks were unchangeable in shape as several times and detected at $2\theta = 44.5, 51.8,$ and $76.4°$. However, higher and sharper intensity peak of metallic Ni was found with increasing temperature. The results also show that the intensity peak of coke was weaker and broader by increasing temperature and oxygen content.

The XRD pattern of spent catalysts under steady state operation at different oxygen contents and reaction temperatures show similar trend as periodic operation. Table 5.2 shows the crystalline sizes of nickel and deposited coke at different conditions by using Scherrer equation for calculation. It was found that at higher temperature, larger crystalline size of both nickel and coke were observed. These results were corresponding to those from BET surface area; larger crystalline size of particle induced to be lessened BET surface area.
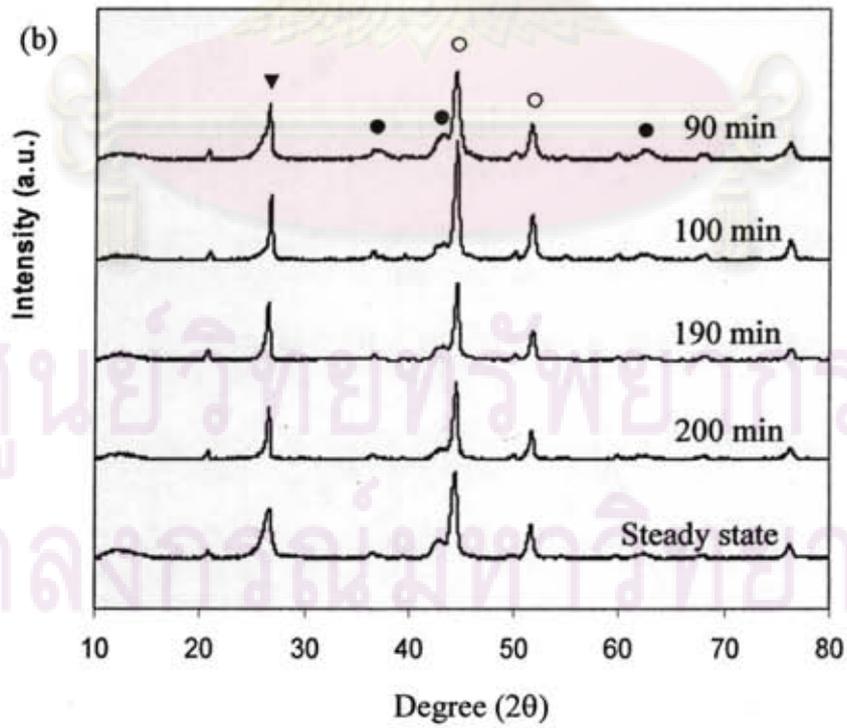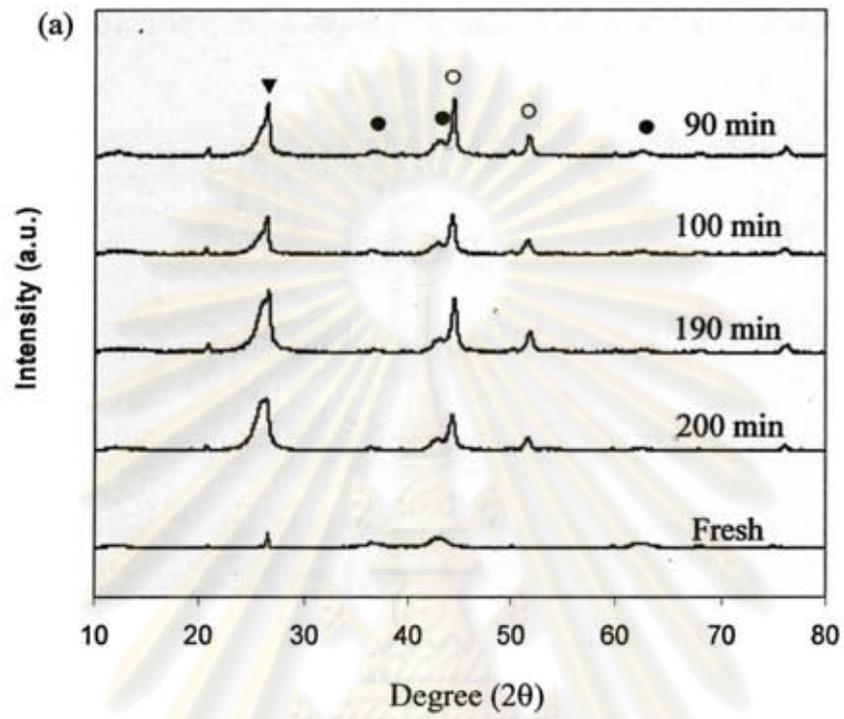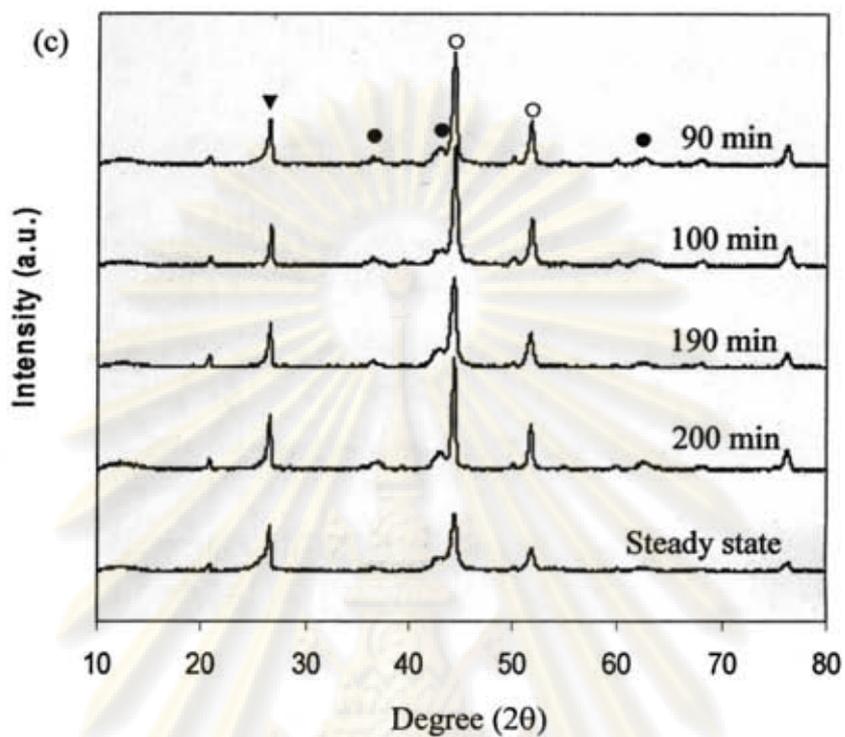
Figure 5.15 XRD patterns of spent catalysts after exposure in the reaction at $650^{\circ}C$ with different reactant ratios and reaction times under periodic and steady state operation (a) no O_2 (b) $CO_2:O_2=9:1$ (c) $CO_2:O_2=7:3$ ▼ Coke ○ Ni ● NiO
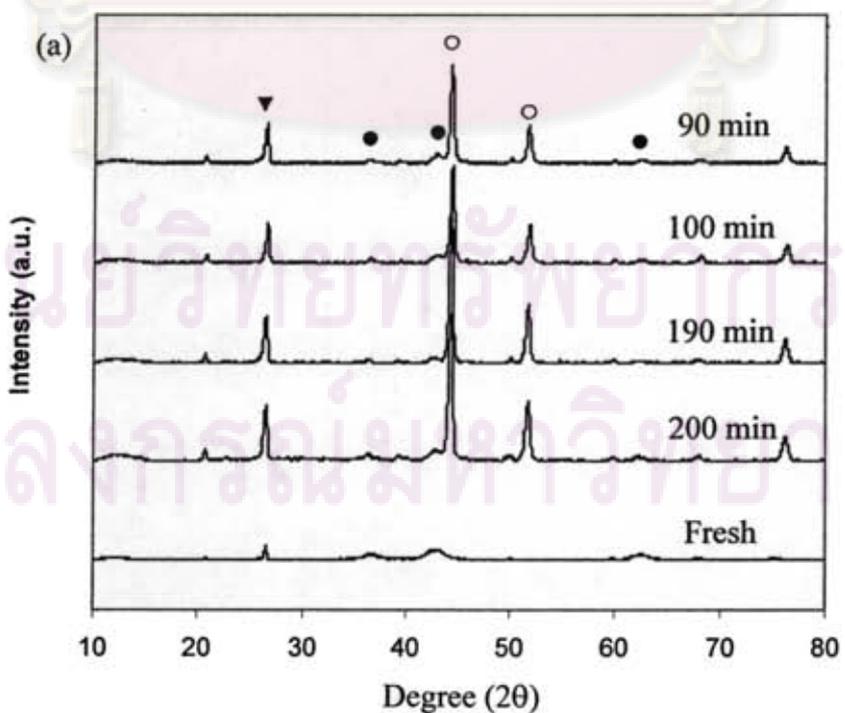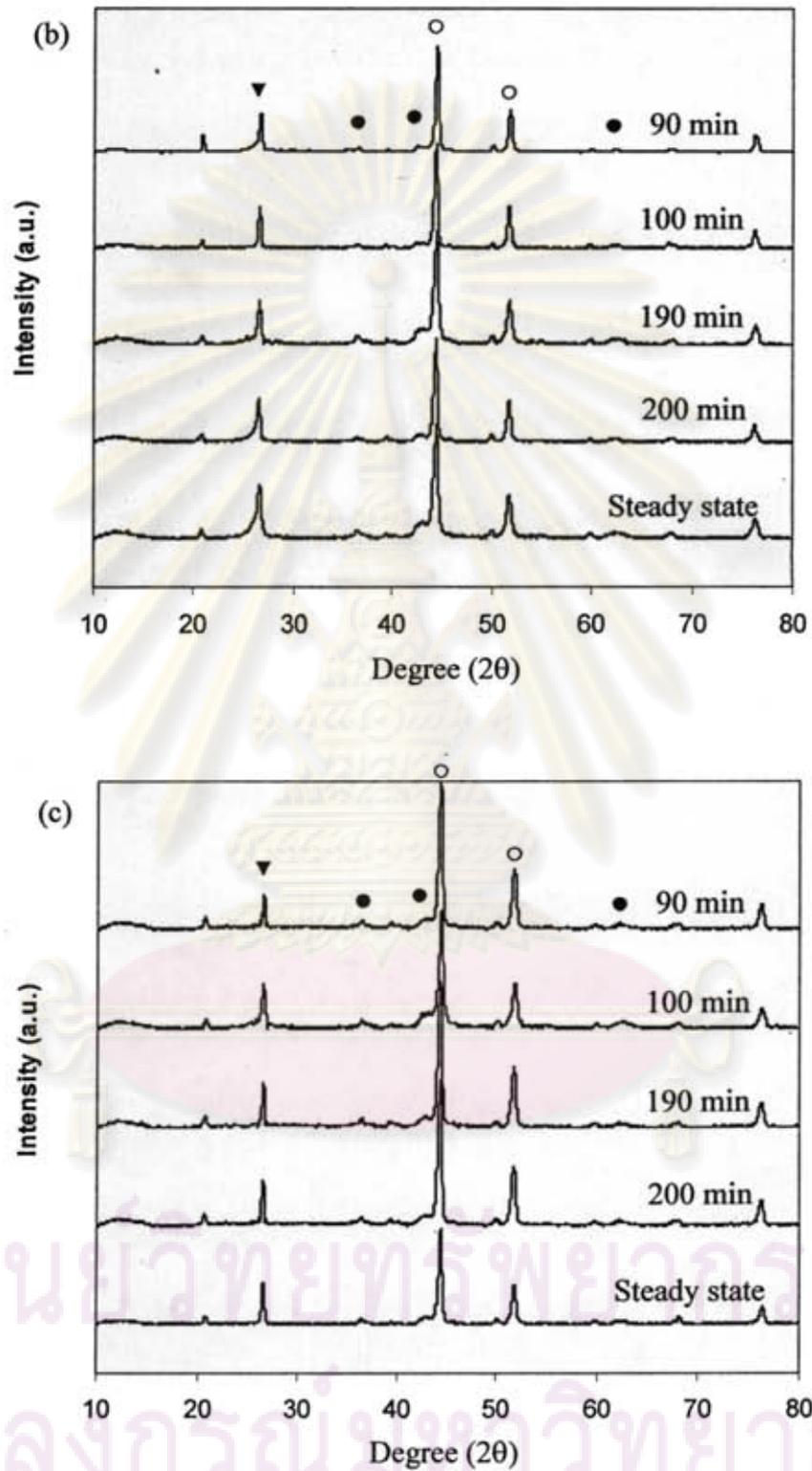
Figure 5.16 XRD patterns of spent catalysts after exposure in the reaction at 750°C with different reactant ratios and reaction times under periodic and steady state operation (a) no O_2 (b) $CO_2:O_2=9:1$ (c) $CO_2:O_2=7:3$ ▼ Coke ○ Ni ● NiO

Table 5.2 The crystalline sizes of coke deposited on catalysts at different conditions

| Catalysts			d-spacing of coke (nm)			
Rxn.Temp.	Oxidant ratio	Operation	Rxn. time			
			90min	100min	190min	200min
650°C	No O_2	Periodic	9.82	15.69	17.66	5.73
	$CO_2:O_2=9:1$	Steady state	-	-	-	14.39
		Periodic	17.43	20.83	19.53	15.6
	$CO_2:O_2=7:3$	Steady state	-	-	-	17.25
		Periodic	18.38	22.14	16.78	20.44
750°C	No O_2	Periodic	35.75	39.34	27.36	26.1
	$CO_2:O_2=9:1$	Steady state	-	-	-	35.84
		Periodic	30.88	35.76	33.76	36.74
	$CO_2:O_2=7:3$	Steady state	-	-	-	39.64
		Periodic	37.55	39.85	36.94	38.34

Table 5.3 The crystalline sizes of nickel on catalysts at different conditions

Catalysts			d-spacing of nickel (nm)			
Fresh			4.83			
After calcination in air at 750 °C 3 hr			25.45			
After calcination and reduction with H_2 at 750 °C 1 hr			21.11			
Rxn.Temp.	Oxidant ratio	Operation	Rxn. time			
			90min	100min	190min	200min
650°C	No O_2	Periodic	18.23	14.96	14.9	13.86
	$CO_2:O_2=9:1$	Steady state	-	-	-	15.67
		Periodic	14.76	16.23	14.93	17.34
	$CO_2:O_2=7:3$	Steady state	-	-	-	18.55
		Periodic	15.53	13.65	12.65	12.82
750°C	No O_2	Periodic	26.88	28.25	20.9	27.92
	$CO_2:O_2=9:1$	Steady state	-	-	-	30.45
		Periodic	27.45	30.02	27.49	28.76
	$CO_2:O_2=7:3$	Steady state	-	-	-	26.84
		Periodic	30.51	27.34	26.47	28.84

Temperature-programmed oxidation (TPO) was used to evaluate the coke on catalyst by burning with oxygen flow to form carbon dioxide. The TPO profiles of spent catalysts under periodic operation with different oxygen contents and reaction temperatures are shown in Figures 5.17-5.18. After the cracking step, peak of coke was detected at lower oxidizing temperature than that after the regeneration step. This indicates that some of coke was previously removed by carbon dioxide and oxygen in the regeneration step but the remainder was difficult to be oxidized.

The amount of deposited coke on catalyst surface was calculated from area beneath curve as shown in Table 5.4. This result was corresponding to all of above measurements. It should be noted that the peaks of coke after regeneration appears at higher temperatures than those after the cracking. This also supports that the remained coke is a difficult-to-oxidize one.
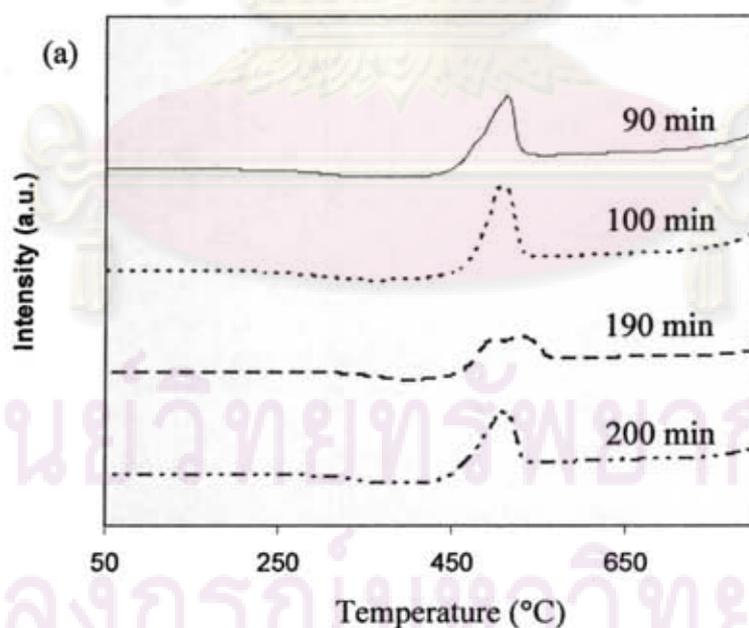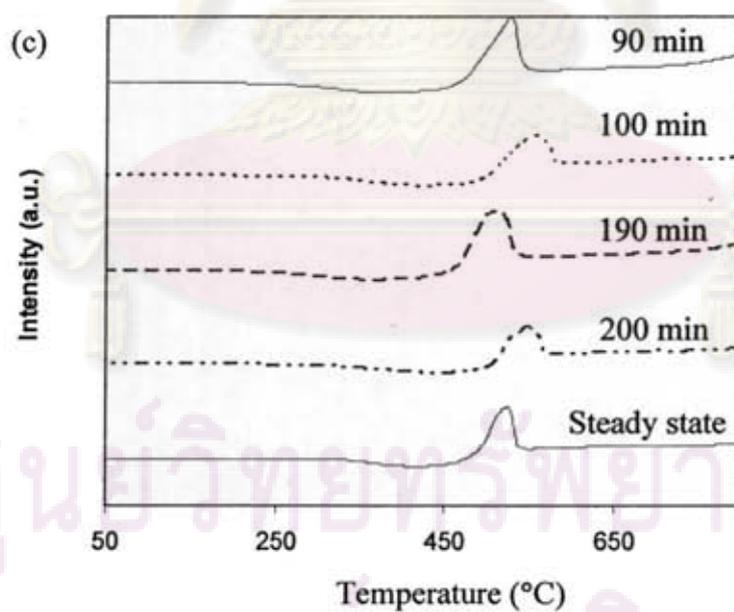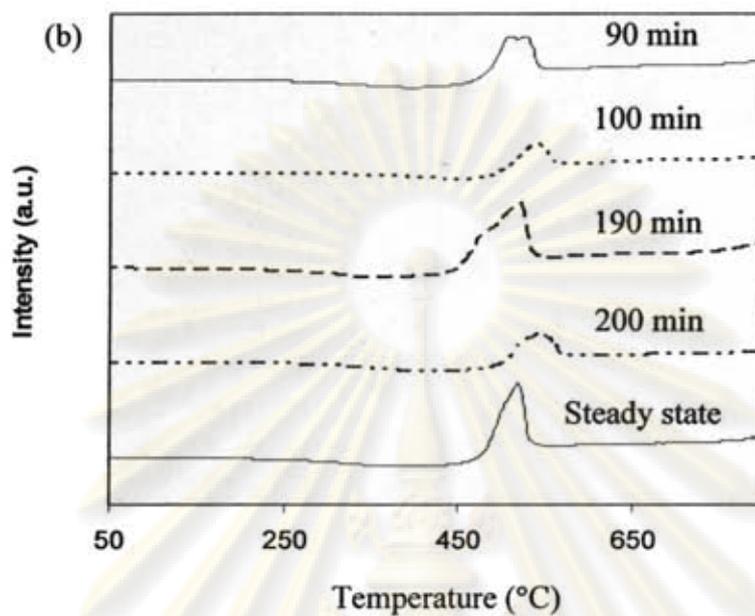
Figure 5.17 TPO profiles of spent catalysts after exposure in the reaction at 650°C with different reactant ratios and reaction times under periodic and steady state operation (a) No O_2 (b) $CO_2:O_2=9:1$ (c) $CO_2:O_2=7:3$
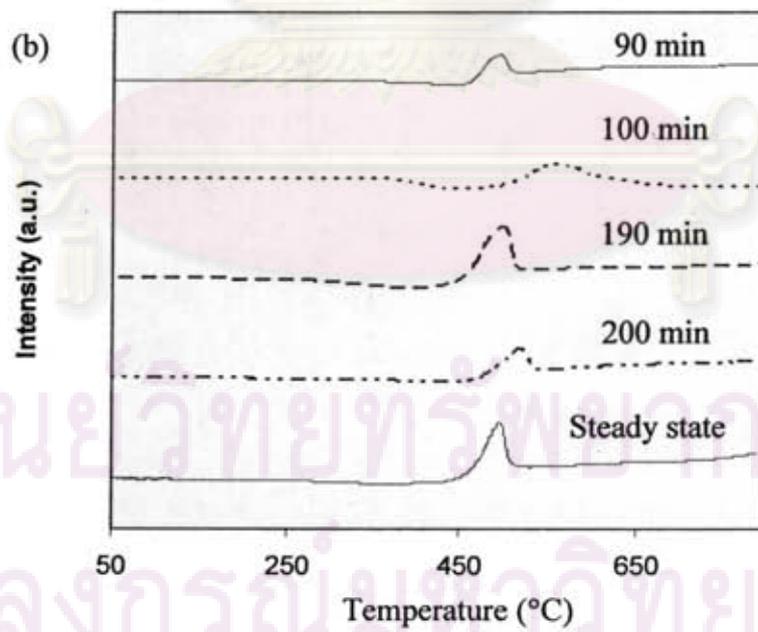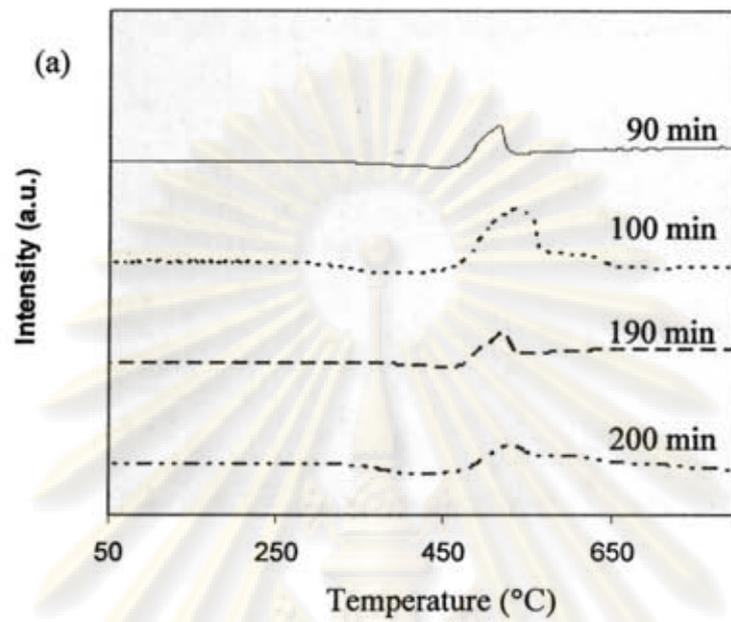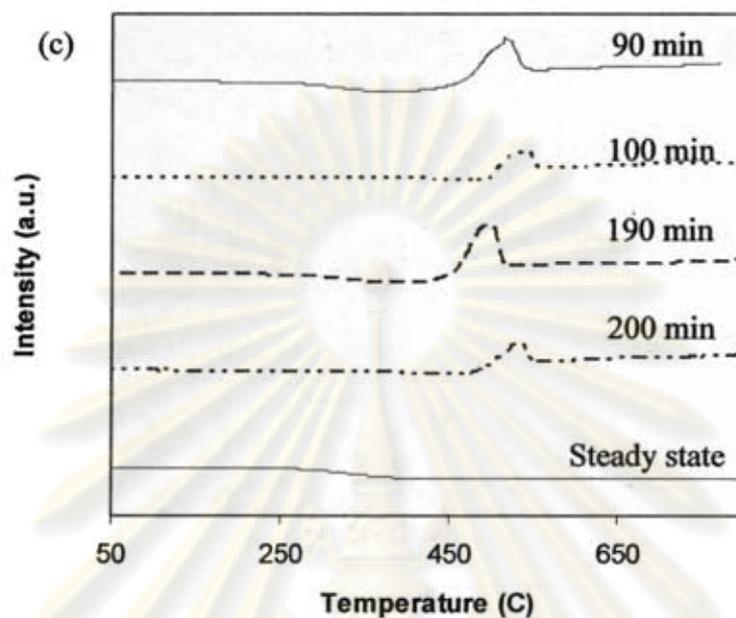
Figure 5.18 TPO profiles of spent catalysts after exposure in the reaction at 750°C with different reactant ratios and reaction times under periodic and steady state operation (a) No O_2 (b) CO_2:O_2=9:1 (c) CO_2:O_2=7:3

Table 5.4 Coke amount obtained from TPO profiles of spent catalysts at different conditions

| Catalysts | | | | Coke amount | |
Rxn.Temp.(°C)	Oxidant ratio	Operation	Rxn. Time (min)	Oxidizing Temp.(°C)	Amount (mg)
650 °C	no O_2	Periodic	90	514.7	5.38
			100	510.1	5.30
			190	529.3	3.88
			200	511.5	4.81
	$CO_2:O_2=9:1$	Steady state	200	519.2	4.74
		Periodic	90	518.6	2.54
			100	551.2	1.33
			190	520.4	5.15
			200	550.3	1.96
	$CO_2:O_2=7:3$	Steady state	200	520.1	2.90
		Periodic	90	524.1	4.73
			100	551.5	3.54
			190	520.8	5.28
			200	546.7	2.88
750 °C	no O_2	Periodic	90	516.2	2.04
			100	538.5	5.30
			190	518.6	1.60
			200	530.4	1.43
	$CO_2:O_2=9:1$	Steady state	200	498.4	2.14
		Periodic	90	503.8	1.02
			100	555.3	0.88
			190	504.2	3.64
			200	523.5	1.15
	$CO_2:O_2=7:3$	Steady state	200	-	-
		Periodic	90	517.8	1.82
			100	546.1	0.85
			190	483.2	3.56
			200	540.4	0.93

5.3 Effects of cycle period and cycle split on reaction performance

In this part, performances of combined carbon dioxide reforming and partial oxidation of methane under periodic operation were investigated using various as cycle periods (τ) and cycle splits (s). All experiments were performed using CO_2/O_2 flow rate ratio of 9/1 at 650°C. In order to investigate the effect of cycle period, the constant cycle split of 0.5 was conducted. From previous study by Promaros et al. (2006), the cracking step was limited at 20 minutes for preventing complete deactivation of catalyst. Therefore, the cycle period was varied at 40 minutes (5 cycles), 20 minutes (10 cycles), and 10 minutes (20 cycles). The results are shown in Figures 5.19-5.20.

It was found that their performances tend to decrease as the cycle period increased; methane conversions and carbon dioxide conversions were slightly decreased from 55% to 47% and from 34% to 29% respectively, when cycle period increased from 10 minutes to 40 minutes. These may be because of higher coke deposition at very long period. However, their performances are lower than did the steady state operation over all cycle periods.
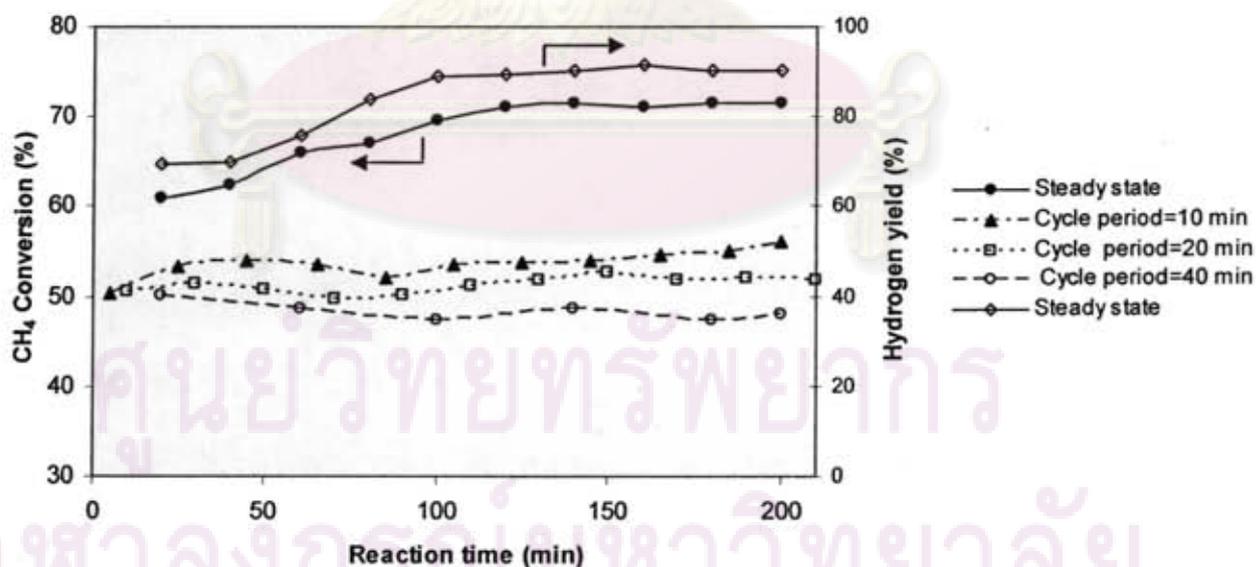
Figure 5.19 Methane conversions comparison between periodic and steady state operation at different cycle periods.
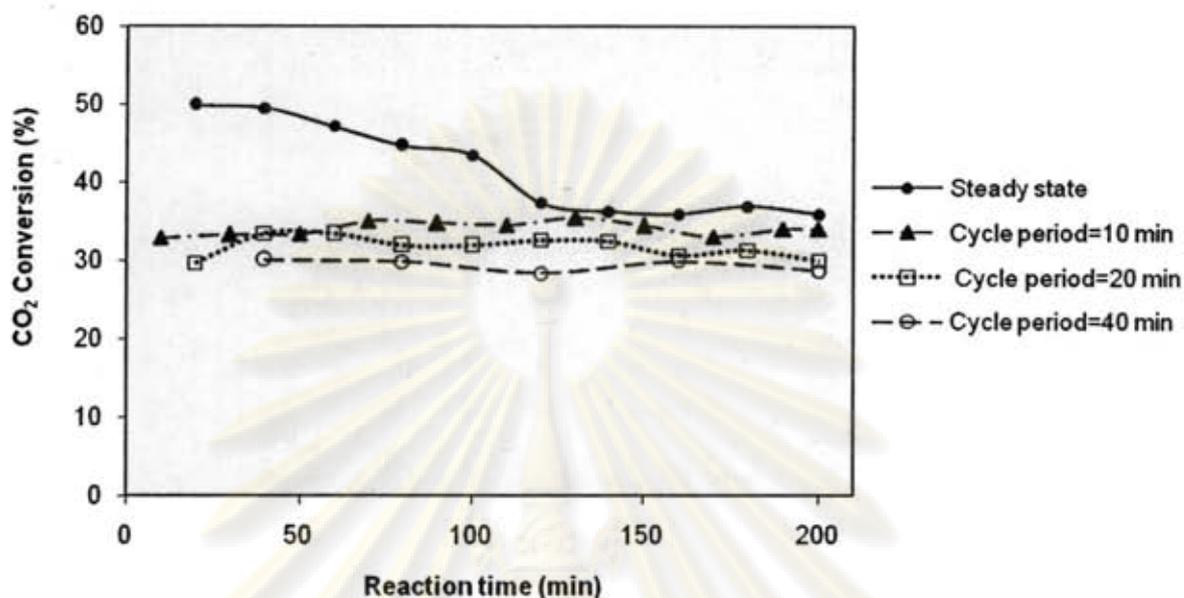
Figure 5.20 Carbon dioxide conversions comparison between periodic and steady state operation at different cycle periods.

Another set of experiments were carried out at constant cycle period of 20 minutes, three values of cycle split at 0.25, 0.5 and 0.75 were considered. The results show that the decrease of the cycle split value from 0.5 to 0.25, both methane and carbon dioxide conversions were slightly decreased from 51% to 44% and from 29% to 26% respectively as a result of the shorter residence time during the methane cracking which caused the lower methane conversion. While the decrease of carbon dioxide conversion due to the higher effect of mass transfer resistance at low reactant flow rate. For using the cycle split value of 0.75, methane conversion and carbon dioxide conversion showed the initial value about 50% and 27% respectively, then conversion further decreased rapidly to 29% and 18% respectively, as shown in Figures 5.21-5.22. This lowest performance is affected by higher amount of coke accumulation because catalyst surface is not fully re-oxidized caused by the decrease in amount of oxygen and carbon dioxide adsorbed on the surface. The performance shows a maximum for a split value of 0.5. It corresponds to asymmetric period when the time of cracking is equal to the time of regeneration due to the same reaction rate of methane cracking and coke oxidation.
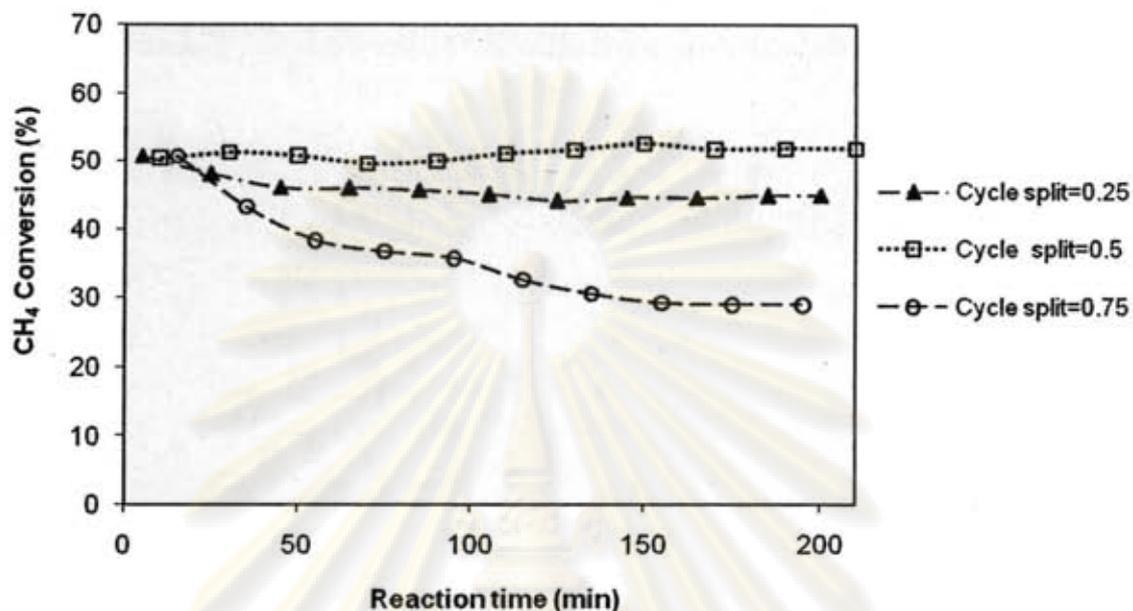
**Figure 5.21** Methane conversions under period operation at different cycle splits.
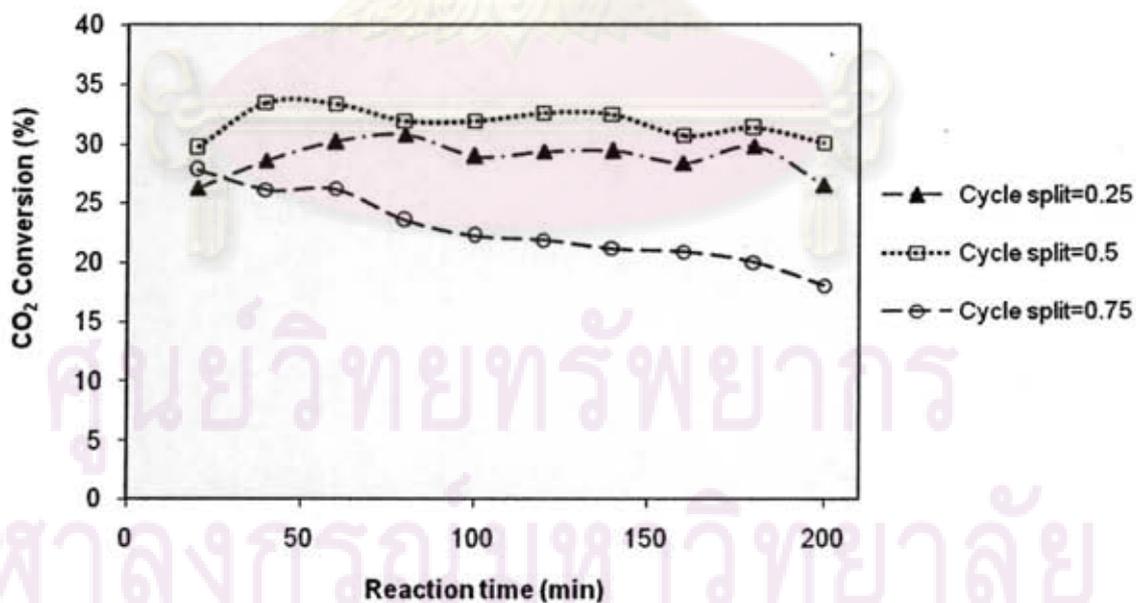
Figure 5.22 Carbon dioxide conversions under period operation at different cycle splits.

CHAPTER VI
CONCLUSIONS AND RECOMMENDATIONS

In this chapter, Section 6.1 provides the conclusions obtained from the experimental studies on reaction performance and spent catalyst characterization of combined carbon dioxide reforming and partial oxidation of methane over $Ni/SiO_2.MgO$ catalyst under periodic and steady state operation at reaction temperature of 650 and 750°C. Additionally, recommendations for further study are given in Section 6.2.

6.1 Conclusions

1. For steady state operation, the catalytic performance of combined carbon dioxide reforming and partial oxidation of methane over $Ni/SiO_2.MgO$ catalyst at reaction temperatures of 650 and 750°C tended to increase with increasing oxygen content and reaction temperature. However, the higher oxygen contents caused slightly decrease in hydrogen yield for both temperatures.

2. For periodic operation, the addition of oxygen into the carbon dioxide reforming of methane at 750°C was able to improve the catalytic stability in terms of methane conversion. Considering the obtained hydrogen yield, it was found that the periodic operation offered the hydrogen yield close to that of the steady state operation at 650°C. In the addition, the periodic operation also provides another benefit on the separated product streams of hydrogen and carbon monoxide.

3. The lower amount of coke was formed on the catalyst surface after exposure to the combined reactions at higher oxygen content and reaction temperature for both periodic and steady state operations.

4. The results showed the optimum performance at cycle period and cycle split of 10 min and 0.5 respectively. This indicated that the rate of methane cracking is equal to the rate of carbon oxidation for this combined process.

6.2 Recommendations

1. The combined carbon dioxide reforming and partial oxidation of methane should be conducted using wider ranges of the manipulated variables such as reaction temperature, $CH_4:CO_2:O_2$ ratios, flow rate and total pressure in order to determine the best condition for synthesis gas production. In addition, the periodic operating parameters like cycle time and cycle split should be investigated in more details.

2. Comparison results between the experiment and the mathematical models are also recommended to investigate the behavior of the system.
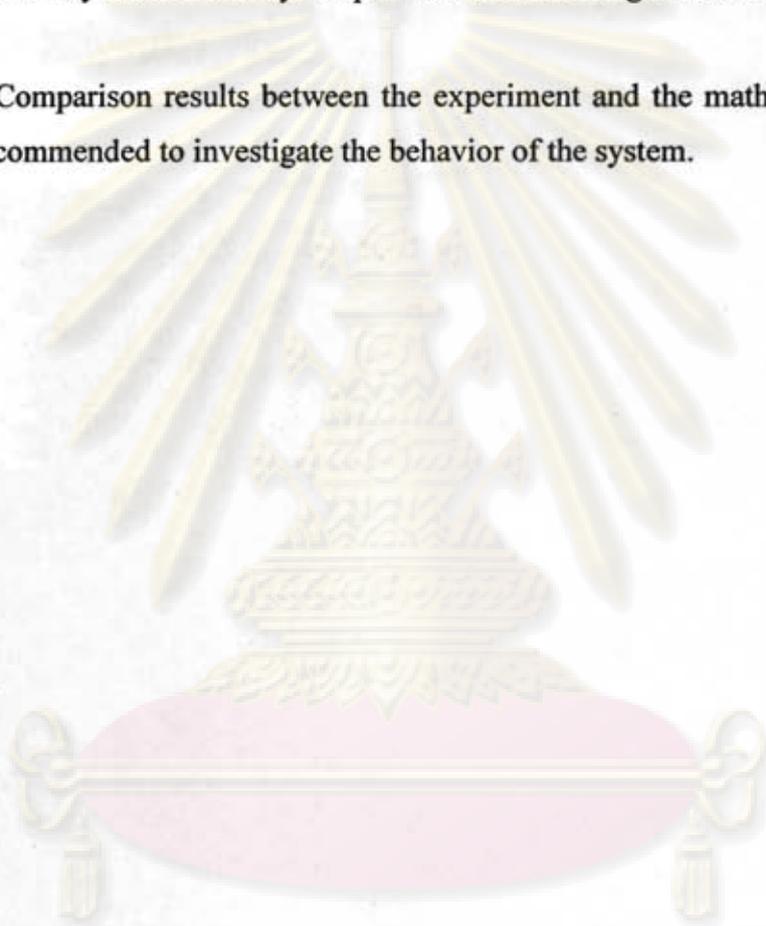
REFERENCES

Aiello, R., Fiscus, J. E., zur Loye, H.-C., and Amiridis, M. D. (2000). "Hydrogen production via the direct cracking of methane over Ni/SiO₂: catalyst deactivation and regeneration." *Applied Catalysis A: General*, 192(2), 227-234.

Amin, N. A. S., and Yaw, T. C. (2007). "Thermodynamic equilibrium analysis of combined carbon dioxide reforming with partial oxidation of methane to syngas." International Journal of Hydrogen Energy, xxx, xxx-xxx.

Ayabe, S., Omoto, H., Utaka, T., Kikuchi, R., Sasaki, K., Teraoka, Y., and Eguchi, K. (2003). "Catalytic autothermal reforming of methane and propane over supported metal catalysts." *Applied Catalysis A: General*, 241, 261-269.

Basile, F., Fornasari, G., Poluzzi, E., and Vaccari, A. (1998). "Catalytic partial oxidation and CO₂-reforming on Rh- and Ni-based catalysts obtained from hydrotalcite-type precursors." *Applied Clay Science*, 13(5-6), 329-345.

Chan, S.H., and Wang, H.M. (2001). "Carbon monoxide yield in natural gas autothermal reforming process." *Journal of Power Sources*, 101, 188-195.

Chang, J.-S., Hong, D.-Y., Li, X., and Park, S.-E. (2006). "Thermogravimetric analyses and catalytic behaviors of zirconia-supported nickel catalysts for carbon dioxide reforming of methane." *Catalysis Today*, 115(1-4), 186-190.

Chang, J.-S., Park, S.-E., Yoo, J. W., and Park, J.-N. (2000). "Catalytic Behavior of Supported KNiCa catalyst and Mechanistic consideration for carbon dioxide reforming of methane." *Journal of Catalysis*, 195, 1-11.

Chen, X., Honda, K., and Zhang, Z.-G. (2004). "CO₂-CH₄ reforming over NiO/γ-Al₂O₃ in fixed-bed/fluidized-bed switching mode." *Catalysis Today*, 93-95, 87-93.

Choudhary, V. R., and Mondal, K. C. (2006). "CO2 reforming of methane combined with steam reforming or partial oxidation of methane to syngas over NdCoO3 perovskite-type mixed metal-oxide catalyst." *Applied Energy*, 83, 1024-1032.

Diaz, K., Garcia, V., and Matos, J. (2007). "Activated carbon supported Ni-Ca: Influence of reaction parameters on activity and stability of catalyst on methane reformation." *Journal of Fuel*, 86(9), 1337-1344.

Djaidja, A., Libs, S., Kiennemann, A., and Barama, A. (2006). "Characterization and activity in dry reforming of methane on NiMg/Al and Ni/MgO catalysts." *Catalysis Today*, 113(3-4), 194-200.

Edwards, J. H., Maitra, A. M. (1995). "The chemistry of methane reforming with carbon dioxide and its current and potential applications." *Fuel Processing Technology*, 42, 269-289.

Ermakova, M. A., and Ermakov, D. Y. (2002). "Ni/SiO$_2$ and Fe/SiO$_2$ catalysts for production of hydrogen and filamentous carbon via methane decomposition." *Catalysis Today*, 77(3), 225-235.

Ferreira-Aparicio, P., Guerrero-Ruiz, A., and Rodriguez-Ramos, I. (1998). "Comparative study at low and medium reaction temperatures of syngas production by methane reforming with carbon dioxide over silica and alumina supported catalysts." *Applied Catalysis A: General*, 170, 177-187.

Galvita, V., and Sundmacher, K. (2005). "Hydrogen production from methane by steam reforming in a periodically operated two-layer catalytic reactor." *Applied Catalysis A: General*, 289(2), 121-127.

Glockler, B., Kolios, G., and Eigenberger, G. (2003). "Analysis of a novel reverse-flow reactor concept for autothermal methane steam reforming." *Chemical Engineering Science*, 58(3-6), 593-601.

Gosiewski, K. (2000). "Mathematical simulations of reactors for catalytic conversion of methane to syngas with forced concentration cycling." *Chemical Engineering and Processing*, 39(5), 459-469.

Guo, J., Lou, H., and Zheng, X. (2007). "The deposition of coke from methane on a Ni/MgAl$_2$O$_4$ catalyst." *Carbon*, xxx, xxx-xxx.

He, Y., and He, Y. (2002). "Characterization of coke precursor deposited on the surface of heteropoly acid catalyst in alkylation." *Catalysis Today*, 74(1-2), 45-51.

Hou, Z., and Yashima, T. (2004). "Meso-porous Ni/Mg/Al catalysts for methane reforming with CO$_2$." *Applied Catalysis A: General*, 261(2), 205-209.

Ito, M., Tagawa, T., and Goto, S. (1999). "Partial oxidation of methane on supported nickel catalysts." *Journal of Chemical Engineering of Japan*, 32, 274-279.

Ito, M., Tagawa, T., and Goto, S. (1999). "Suppression of carbonaceous depositions on nickel catalyst for the carbon dioxide reforming of methane." *Applied Catalysis A: General*, 177(1), 15-23.

Juan-Juan, J., Roman-Martinez, M. C., and Illan-Gomez, M. J. (2004). "Catalytic activity and characterization of Ni/Al_2O_3 and NiK/Al_2O_3 catalysts for CO_2 methane reforming." *Applied Catalysis A: General*, 264(2), 169-174.

Juan-Juan, J., Roman-Martinez, M. C., and Illan-Gomez, M. J. (2006). "Effect of potassium content in the activity of K-promoted Ni/Al_2O_3 catalysts for the dry reforming of methane." *Applied Catalysis A: General*, 301(1), 9-15.

Jing, Q., Lou, H., Fei, J., Hou, Z., and Zheng, X. (2004). "Syngas production from reforming of methane with CO_2 and O_2 over $Ni/SrO-SiO_2$ catalysts in a fluidized bed reactor." *International Journal of Hydrogen Energy*, 29, 1245-1251.

Jing, Q., Lou, H., Mo, L., Fei, J., and Zheng, X. (2004). "Combination of CO2 reforming and partial oxidation of methane over Ni/BaO-SiO2 catalysts to produce low H2/CO ratio syngas using a fluidized bed reactor." *Journal of Molecular Catalysis A: Chemical*, 212, 211-217.

Jing, Q., Lou, H., Mo, L., and Zheng, X. (2006). "Comparative study between fluidized bed and fixed bed reactors in methane reforming with CO_2 and O_2 to produce syngas." *Energy Conversion and Management*, 47, 459-469.

Jing, Q. S., Fei, J. H., Lou, H., Mo, L. Y., and Zheng, X. M. (2004). "Effective reforming of methane with CO2 and O2 to low H2/CO ratio syngas over Ni/MgO-SiO2 using fluidized bed reactor." *Energy Conversion and Management*, 45, 3127-3137.

Jing, Q. S., and Zheng, X. M. (2006). "Combined catalytic partial oxidation and CO2 reforming of methane over ZrO2-modified Ni/SiO2 catalysts using fluidized-bed reactor." *Energy*, 31, 2184-2192.

Koh, A. C. W., Chen, L., Leong, W. K., Johnson, B. F. G., Khimyak, and T., Lin, J. (2007). "Hydrogen or synthesis gas production via the partial oxidation of methane over supported nickel-cobalt catalysts." *International Journal of Hydrogen Energy*, 32, 725-730.

Larentis, A. L., Resende, N. S., Salim, V. M. M., Pinto, and J.C. (2001). "Modeling and optimization of the combined carbon dioxide reforming and partial oxidation of natural gas." *Applied Catalysis A: General*, 215, 211-224.

Lee, S.-H., Cho, W., Ju, W.-S., Cho, B.-H., Lee, Y.-C., and Baek, Y.-S. (2003). "Tri-reforming of CH_4 using CO_2 for production of synthesis gas to dimethyl ether." *Catalysis Today*, 87(1-4), 133-137.

Liu, S., Xiong, G., Dong, H., and Yang, W. (2000). "Effect of carbon dioxide on the reaction performance of partial oxidation of methane over a LiLaNiO/γ-Al_2O_3 catalys." *Applied Catalysis A: General*, 202, 141-146.

Matsumura, Y., and Nakamori, T. (2004). "Steam reforming of methane over nickel catalysts at low reaction temperature." *Applied Catalysis A: General*, 258(1), 107-114.

Mo, L., Fei, J., Huang, C., and Zheng, X. (2003). "Reforming of methane with oxygen and carbon dioxide to produce syngas over a novel $Pt/CoAl_2O_4/Al_2O_3$ catalyst." *Journal of Molecular Catalysis A: chemical*, 193, 177-184.

Monnerat, B., Kiwi-Minsker, L., and Renken, A. (2001). "Hydrogen production by catalytic cracking of methane over nickel gauze under periodic reactor operation." *Chemical Engineering Science*, 56(2), 633-639.

O'Connor, A. M., and Ross, J.R.H. (1998). "The effect of O_2 addition on the carbon dioxide reforming of methane over Pt/ZrO_2 catalysts." *Catalysis Today*, 46, 203-210.

Opoku-Gyamfi, K., and Adesina, A. A. (1999). "Forced composition cycling of a novel thermally self-sustaining fluidised-bed reactor for methane reforming." *Chemical Engineering Science*, 54(13-14), 2575-2583.

Opoku-Gyamfi, K., Vieira-Dias, J., and Adesina, A. A. (2000). "Influence of cycle parameters on periodically operated fluidised bed reactor for CH_4 autoreforming." *Catalysis Today*, 63(2-4), 507-515.

Pawelec, B., Damyanova, S., Arishtirova, K., Fierro, J. L. G., and Petrov, L. (2007). "Structural and surface features of PtNi catalysts for reforming of methane with CO_2." *Applied Catalysis A: General*, 323, 188-201.

Pompeo, F., Nichio, N. N., Gonzalez, M. G., and Montes, M. (2005). "Characterization of Ni/SiO_2 and Ni/Li-SiO_2 catalysts for methane dry reforming." *Catalysis Today*, 107-108, 856-862.

Promaros, E., Assabumrungrat, S., Laosiripojana, N., Praserthdam, P., Tagawa, T., and Goto, S. (2007). "Carbon dioxide reforming of methane under periodic operation." *Korean Journal of Chemical Engineering*, 24(1), 44-50.

Rakass, S., Oudghiri-Hassani, H., Rowntree, P., and Abatzoglou, N. (2006). "Steam reforming of methane over unsupported nickel catalysts." *Journal of Power Sources*, 158(1), 485-496.

Roh, H.-S., Potdar, H. S., and Jun, K.-W. (2004). "Carbon dioxide reforming of methane over co-precipitated Ni-CeO$_2$, Ni-ZrO$_2$ and Ni-Ce-ZrO$_2$ catalysts." *Catalysis Today*, 93-95, 39-44.

Rostrup-Nielsen, J. R., and Hansen, J.-H. B. (1993). "CO$_2$-reforming of methane over transition metals." *Journal of Catalysis*, 144, 38-49.

Sahoo, S. K., Rao, P. V. C., Rajeshwer, D., Krishnamurthy, K. R., and Singh, I. D. (2003). "Structural characterization of coke deposits on industrial spent paraffin dehydrogenation catalysts." *Applied Catalysis A: General*, 244(2), 311-321.

Shamsi, A., Baltrus, J. P., and Spivey, J. J. (2005). "Characterization of coke deposited on Pt/alumina catalyst during reforming of liquid hydrocarbons." *Applied Catalysis A: General*, 293, 145-152.

Silveston, P., Hudgins, R. R., and Renken, A. (1995). "Periodic operation of catalytic reactors-introduction and overview." *Catalysis Today*, 25, 91-112.

Slagtern, A., Olsbye, U., Blom, R., Dahl, I. M., and Fjellvag, H. (1996). "In situ XRD characterization of La---Ni---Al---O model catalysts for CO$_2$ reforming of methane." *Applied Catalysis A: General*, 145(1-2), 375-388.

Snoeck, J. W., Froment, G. F., and Fowles, M. (1997a). "Filamentous Carbon Formation and Gasification: Thermodynamics, Driving Force, Nucleation, and Steady-State Growth." *Journal of Catalysis*, 169(1), 240-249.

Snoeck, J. W., Froment, G. F., and Fowles, M. (1997b). "Kinetic Study of the Carbon Filament Formation by Methane Cracking on a Nickel Catalyst." *Journal of Catalysis*, 169(1), 250-262.

Song, X., and Guo, Z. (2006). "Technologies for direct production of flexible H$_2$/CO synthesis gas." *Energy Conversion and Management*, 47, 560-569.

Souza, M. d. M. V. M., Clave, L., Dubois, V., Perez, C. A. C., and Schmal, M. (2004). "Activation of supported nickel catalysts for carbon dioxide reforming of methane." *Applied Catalysis A: General*, 272(1-2), 133-139.

Souza, M. M. V. M., and Schmal, M. (2003). "Combination of carbon dioxide reforming and partial oxidation of methane over supported platinum catalysts." *Applied Catalysis A: General*, 255(1), 83-92.

Sturzenegger, M., D'Souza, L., Struis, R. P. W. J., and Stucki, S. (2006). "Oxygen transfer and catalytic properties of nickel iron oxides for steam reforming of methane." *Fuel*, 85(10-11), 1599-1602.

Takano, A., Tagawa, T., and Goto, S. (1994). "Carbon dioxide reforming of methane on supported nickel catalysts." *Journal of Chemical Engineering of Japan*, 27, 727 -731.

Tomishige, K., Matsuo, Y., Yoshinaga, Y., Sekine, Y., Asadullah, M., and Fujimoto, K. (2002)." *Applied Catalysis A: General*, 223, 225-238.

Tomishige, K., Nurunnabi, M., Maruyama, K., and Kunimori, K. (2004). "Effect of oxygen addition to steam and dry reforming of methane on bed temperature profile over Pt and Ni catalysts." *Fuel Processing Technology*, 85, 1103-1120.

Tsang, S. C., Claridge, J. B., and Green, M. L. H. (1995). "Recent advances in the conversion of methane to synthesis gas." *Catalysis Today*, 23, 3-15.

Tsyganok, A. I., Tsunoda, T., Hamakawa, S., Suzuki, K., Takehira, K., and Hayakawa, T. (2003). "Dry reforming of methane over catalysts derived from nickel-containing Mg-Al layered double hydroxides." *Journal of Catalysis*, 213(2), 191-203.

Valentini, A., Carreno, N. L. V., Probst, L. F. D., Lisboa-Filho, P. N., Schreiner, W. H., Leite, E. R., and Longo, E. (2003). "Role of vanadium in Ni:Al$_2$O$_3$ catalysts for carbon dioxide reforming of methane." *Applied Catalysis A: General*, 255(2), 211-220.

Villacampa, J. I., Royo, C., Romeo, E., Montoya, J. A., Del Angel, P., and Monzon, A. (2003). "Catalytic decomposition of methane over Ni-Al$_2$O$_3$ coprecipitated catalysts: Reaction and regeneration studies." *Applied Catalysis A: General*, 252(2), 363-383.

Wang, Z., Pan, Y., Dong, T., Zhu, X., Kan, T., Yuan, L., Torimoto, Y., Sadakata, M., and Li, Q. (2007). "Production of hydrogen from catalytic steam reforming of

bio-oil using C12A7-O--based catalysts." *Applied Catalysis A: General*, 320, 24-34.

Wei, J., and Iglesia, E. (2004). "Structural requirements and reaction pathways in methane activation and chemical conversion catalyzed by rhodium." *Journal of Catalysis*, 225, 116-127.

Xu, S., Zhao, R., and Wang, X. (2004). "Highly coking resistant and stable Ni/Al_2O_3 catalysts prepared by W/O microemulsion for partial oxidation of methane." *Fuel Processing Technology*, 86, 123-133.

Zhang, J., Schneider, A., and Inden, G. (2003). "Characterisation of the coke formed during metal dusting of iron in $CO-H_2-H_2O$ gas mixtures." *Corrosion Science*, 45(6), 1329-1341.

Zhang, T., and Amiridis, M. D. (1998). "Hydrogen production via the direct cracking of methane over silica-supported nickel catalysts." *Applied Catalysis A: General*, 167(2), 161-172.

Zhang, W. D., Liu, B. S., Zhu, C., and Tian, Y. L. (2005). "Preparation of $La_2NiO_4/ZSM-5$ catalyst and catalytic performance in CO_2/CH_4 reforming to syngas." *Applied Catalysis A: General*, 292, 138-143.

APPENDICES

ศูนย์วิทยทรัพยากร
จุฬาลงกรณ์มหาวิทยาลัย

APPENDIX A

CALCULATION FOR CATALYST PERFORMANCE

An effluent gas was analyzed using 1 mL sample injected into GC to determine its composition. Concentration of each gas sample could be calculated from the calibration curve.

For steady state operation, ($CH_4 + CO_2 \rightarrow 2CO + 2H_2$, $CH_4 + 1/2 O_2 \rightarrow CO + 2H_2$, $CH_4 + 2O_2 \rightarrow CO_2 + 2H_2O$) volumetric flow rate of total reactant inlet (V_{inlet}) was controlled to be 25 mL/min. Volumetric flow rate of total product outlet (V_{outlet}) can be measured from a bubble flow meter. Methane conversion was defined as molar flow rate of methane reacted during the reaction period ($F_{CH_4, reacted}$), with respect to inlet mole flow rate of methane in feed passed through reactor during the reaction period ($F_{CH_4, inlet}$)

$$
\begin{aligned}
CH_4 \ Conversion &= \frac{(F_{CH_4, reacted})}{(F_{CH_4, inlet})} \times 100 \\
&= \frac{(F_{CH_4, inlet} - F_{CH_4, outlet})}{(F_{CH_4, inlet})} \times 100 \\
&= \frac{(C_{CH_4, inlet} V_{inlet} - C_{CH_4, outlet} V_{outlet})}{(C_{CH_4, inlet} V_{inlet})} \times 100 \quad (A.1)
\end{aligned}
$$

Conversion of carbon dioxide and oxygen also could be obtained in a similar way as calculation of methane conversion.

$$
CO_2 \ Conversion = \frac{(C_{CO_2, inlet} V_{inlet} - C_{CO_2, outlet} V_{outlet})}{(C_{CO_2, inlet} V_{inlet})} \times 100 \quad (A.2)
$$

$$
O_2 \ Conversion = \frac{(C_{O_2, inlet} V_{inlet} - C_{O_2, outlet} V_{outlet})}{(C_{O_2, inlet} V_{inlet})} \times 100 \quad (A.3)
$$

Hydrogen and carbon monoxide yield are calculated from molar flow rate of hydrogen respect to molar flow rate of methane inlet.

$$H_2\ Yield = \frac{1}{2} \times \frac{(C_{H_2,outlet}\ V_{outlet})}{(C_{CH_4,inlet}\ V_{outlet})} \times 100 \qquad (A.4)$$

For periodic operation, the main reaction in the reactor could be separated to catalytic cracking of methane ($CH_4 \longrightarrow C+2H_2$) and catalyst regeneration with carbon dioxide and oxygen (C + CO$_2$ ↔ 2CO, C + 1/2O$_2$ → CO, CO +1/2O$_2$→ CO$_2$). A mixture of reactant and product gas from cracking period (CH$_4$, H$_2$) and regeneration period (CO$_2$, O$_2$, CO) would be collected with the sampling bag after finishing each cycle. The conversion of methane in the cracking period and conversion of carbon dioxide and oxygen in the regeneration period for periodic mode could be calculated as follows:

Cracking Period:

$$CH_4\ Conversion = \frac{(F_{CH_4,reacted})}{(F_{CH_4,inlet})} \times 100$$

$$= \frac{(mol\ CH_{4,inlet} - mol\ CH_{4,outlet})}{(molCH_{4,inlet})} \times 100$$

$$= \frac{(mol\ CH_{4,inlet} - molCH_{4,outlet})}{(molCH_{4,inlet} - molCH_{4,outlet} + molCH_{4,outlet})} \times 100$$

$$= \frac{\left(\frac{1}{2} \times molH_{2,outlet}\right)}{\left(\frac{1}{2} \times molH_{2,outlet} + molCH_{4,outlet}\right)} \times 100$$

Multiply by $\dfrac{2}{(molCH_{4,outlet})}$ therefore;

$$CH_4\ Conversion\ (\%) = \frac{\left(\dfrac{molH_{2,outlet}}{molCH_{4,outlet}}\right)}{\left(\dfrac{molH_{2,outlet}}{molCH_{4,outlet}} + 2\right)} \times 100 \qquad (A.5)$$

$$H_2 \; Yield \;\; = \;\; \frac{1}{2} \times \frac{(F_{H_2,outlet})}{(F_{CH_4,inlet})} \times 100$$

$$= \frac{\left(\frac{1}{2} mol H_{2,outlet}\right)}{\left(mol CH_{4,inlet} - mol CH_{4,outlet} + mol CH_{4,outlet}\right)} \times 100$$

$$= \frac{\left(\frac{1}{2} mol H_{2,outlet}\right)}{\left(\frac{1}{2} mol H_{2,outlet} + mol CH_{4,outlet}\right)} \times 100$$

Multiply by $\dfrac{2}{\left(mol CH_{4,outlet}\right)}$ therefore;

$$H_2 \; Yield \; (\%) \;\; = \;\; \frac{\left(\dfrac{mol H_{2,outlet}}{mol CH_{4,outlet}}\right)}{\left(\dfrac{mol H_{2,outlet}}{mol CH_{4,outlet}} + 2\right)} \times 100 \qquad (A.6)$$

Regeneration Period:

$$C + CO_2 \;\; \leftrightarrow \;\; 2CO$$

Extent x

$$C + 1/2O_2 \;\; \rightarrow \;\; CO$$

Extent y

$$CO + 1/2O_2 \;\; \rightarrow \;\; CO_2$$
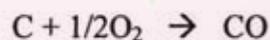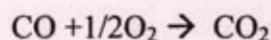
Extent z

$$F_{CO_2} = F_{CO_2,in} - x + z \qquad (1)$$

$$F_{CO} = F_{CO,in} + 2x + y - z \qquad (2)$$

$$F_{O_2} = F_{C_2,in} - 1/2y - 1/2z \qquad (3)$$

From the results, it was found that: $\quad F_{O_2,out} = 0$

From Eq.3; $\qquad 0 = F_{O_2,in} - \dfrac{y}{2} - \dfrac{z}{2}$

Thus, $\qquad z = 2F_{O_2,in} - y$ $\qquad\qquad$ (4)

Substitute (4) into (1) and (2);

$$F_{CO_2} = F_{CO_2,in} - x + 2F_{O_2,in} - y = F_{CO_2,in} + 2F_{O_2,in} - (x+y) \qquad (5)$$

$$F_{CO} = 2x + y - 2F_{O_2,in} + y = 2(x+y) - 2F_{O_2,in} \qquad (6)$$

Let $\Lambda = x + y$

(5)/(6); $\qquad \dfrac{F_{CO_2}}{F_{CO}} = \left(\dfrac{\eta_{CO_2}}{\eta_{CO}}\right)_{measured} = \dfrac{F_{CO_2,in} + 2F_{O_2,in} - \Lambda}{2\Lambda - 2F_{O_2,in}} \qquad (7)$

We know $F_{CO_2,in}$, $F_{O_2,in}$ and $\left(\dfrac{\eta_{CO_2}}{\eta_{CO}}\right)$ in sampling bag, we can calculate Λ

$$CO_2 \; Conversion \quad = \quad \dfrac{(F_{CO_2,reacted})}{(F_{CO_2,inlet})} \times 100$$

From (5);

$$CO_2 Conversion(\%) = \dfrac{\Lambda - 2F_{O_2,in}}{F_{CO_2,in}} \times 100 \qquad (A.7)$$

It was found that $\qquad O_2 Conversion(\%) = 100\%$

APPENDIX B
CALIBRATION CURVES

This appendix shows the calibration curves for calculation of composition of reactant and products in the carbon dioxide reforming of methane reaction. The reactants are carbon dioxide and methane. The products are synthesis gas, containing carbon monoxide and hydrogen.

The Gas chromatography Shimadzu model 8A with a thermal conductivity detector (TCD), was used for analyzing the concentration of all reactants and products by using Molecular sieve 5A column and Porapak-Q column, respectively. Conditions used in for GC analyzing are illustrated in Table B.1.

Mole of reagent in y-axis and area reported by gas chromatography in x-axis are exhibited in the curves. The calibration curves of carbon monoxide, carbon dioxide, methane, and hydrogen are shown in the following figures.

Table B.1 Conditions used in Shimadzu model GC-8A

| Parameters	Condition (Shimadzu GC-8A)
Width	5
Slope	50
Drift	0
Min. area	10
T.DBL	0
Stop time	30
Atten	5
Speed	2
Method	41
Format	1
SPL.WT	100
IS.WT	1
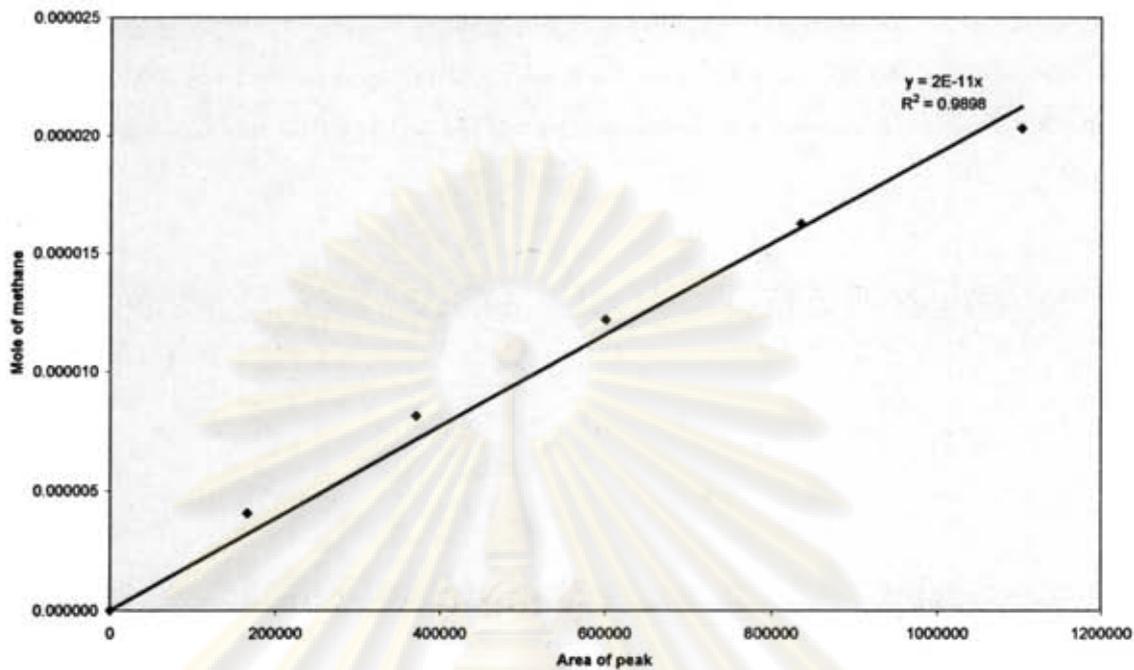
**Figure B.1** The calibration curve of methane
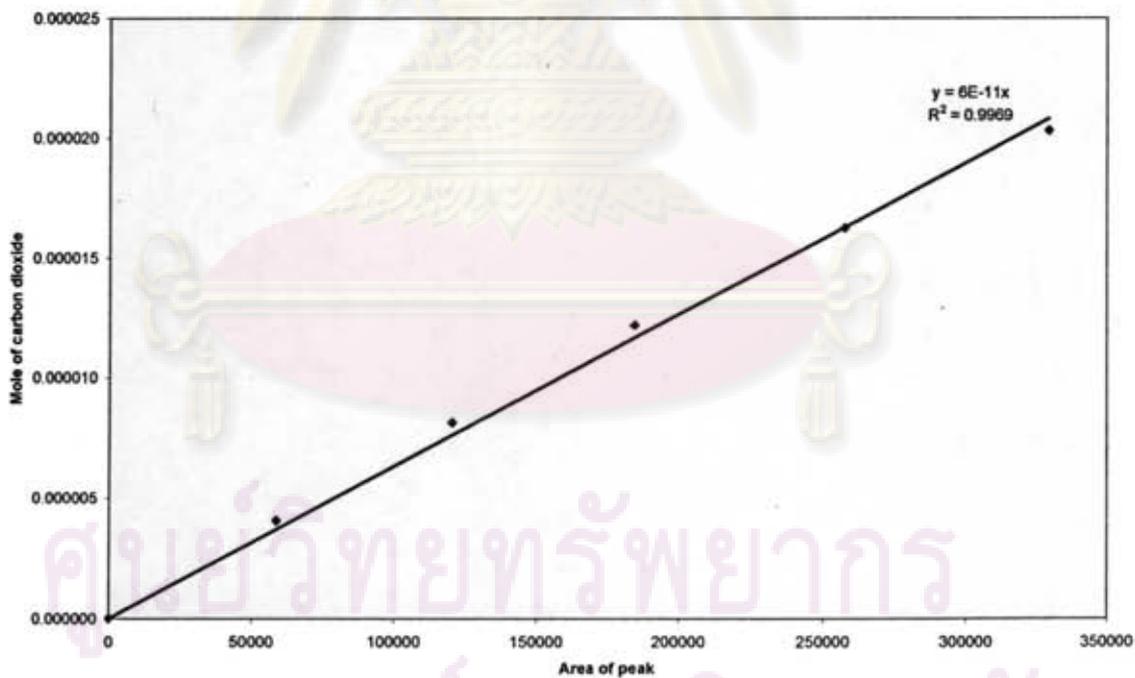
**Figure B.2** The calibration curve of carbon dioxide
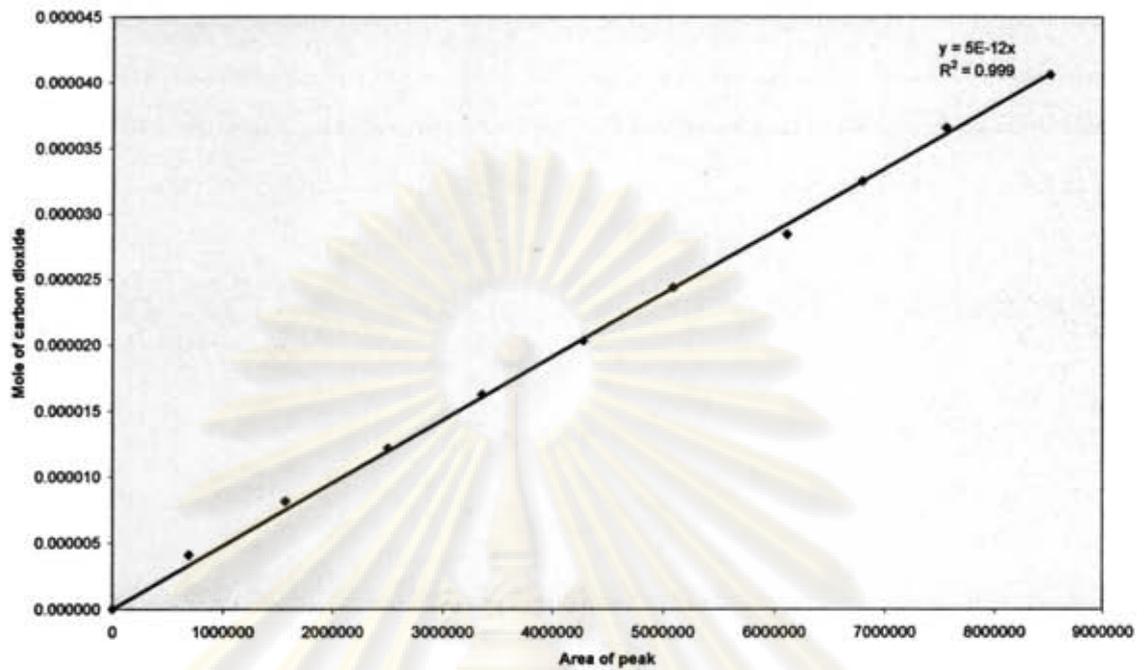
Figure B.3 The calibration curve of hydrogen
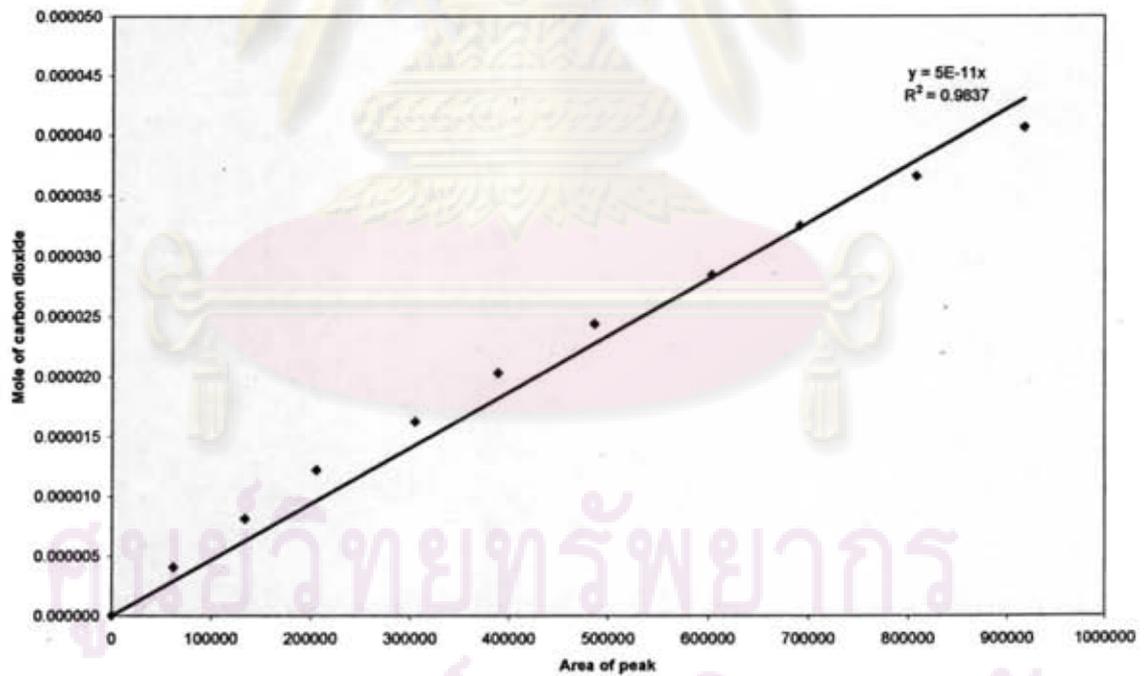
Figure B.4 The calibration curve of carbon monoxide

APPENDIX C

CALCULATION OF THE CRYSTALLITE SIZE

Calculation of the crystallite size by Scherrer equation

The crystallite size was calculated from the half-height width of the diffraction peak of XRD pattern using the Debye-Scherrer equation.

From Scherrer equation:

$$D = \frac{K\lambda}{\beta \cos \theta} \tag{C.1}$$

where D = Crystallite size, Å

           K = Crystallite-shape factor = 0.9

           λ = X-ray wavelength, 1.5418 Å for CuKα

           θ = Observed peak angle, degree

           β = X-ray diffraction broadening, radian

The X-ray diffraction broadening (β) is the pure width of a powder diffraction free of all broadening due to the experimental equipment. Standard α-alumina is used to observe the instrumental broadening since its crystallite size is larger than 2000 Å. The X-ray diffraction broadening (β) can be obtained by using Warren's formula.

From Warren's formula:

$$\beta^2 = B_M^2 - B_S^2 \tag{C.2}$$

$$\beta = \sqrt{B_M^2 - B_S^2}$$

Where B_M = The measured peak width in radians at half peak height.

           B_S = The corresponding width of a standard material.

Example: Calculation of the crystallite size of Ni obtained by spent catalyst after carbon dioxide reforming of methane reaction under periodic operation at reaction temperature 750°C and reaction time 190 min (PO750C190)

The half-height width of peak $= 0.36°$ (from Figure C.1)

$= (2\pi \times 0.36)/360$

$= 0.00628$ radian

The corresponding half-height width of peak of α-alumina $= 0.0038$ radian

The pure width $= \sqrt{B_M^2 - B_S^2}$

$= \sqrt{0.00628^2 - 0.0038^2}$

$= 0.00515$ radian

$\beta = 0.00515$ radian

$2\theta = 26.52°$

$\theta = 13.26°$

$\lambda = 1.5418$ Å

The crystallite size $= \dfrac{0.9 \times 1.5418}{0.00515 \cos 13.26}$

$= 273.64$ Å

$= 27.3$ nm
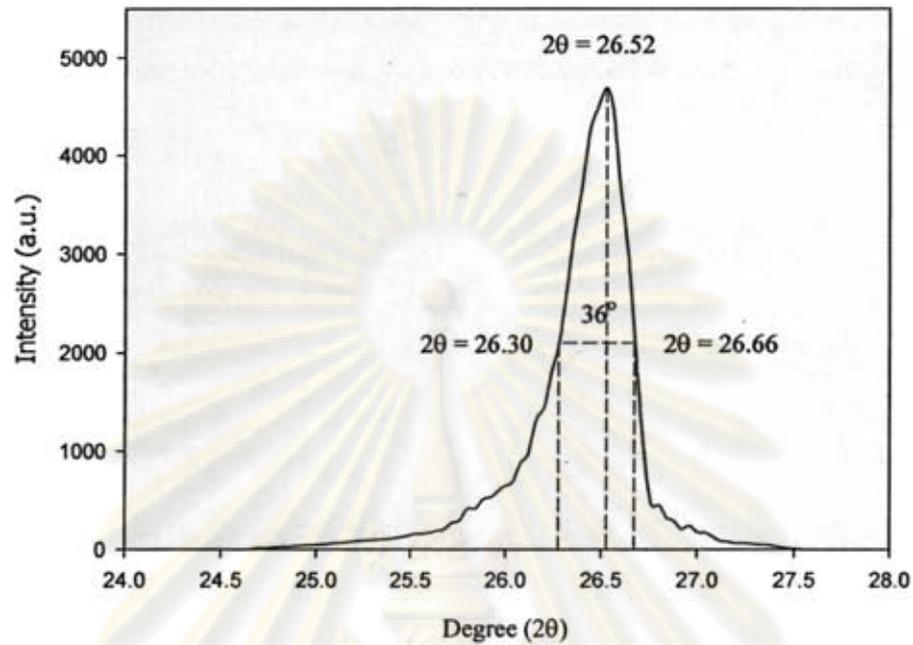
Figure C.1 The measured peak of Ni obtained by spent catalyst (PO750C190) to calculate the crystallite size.
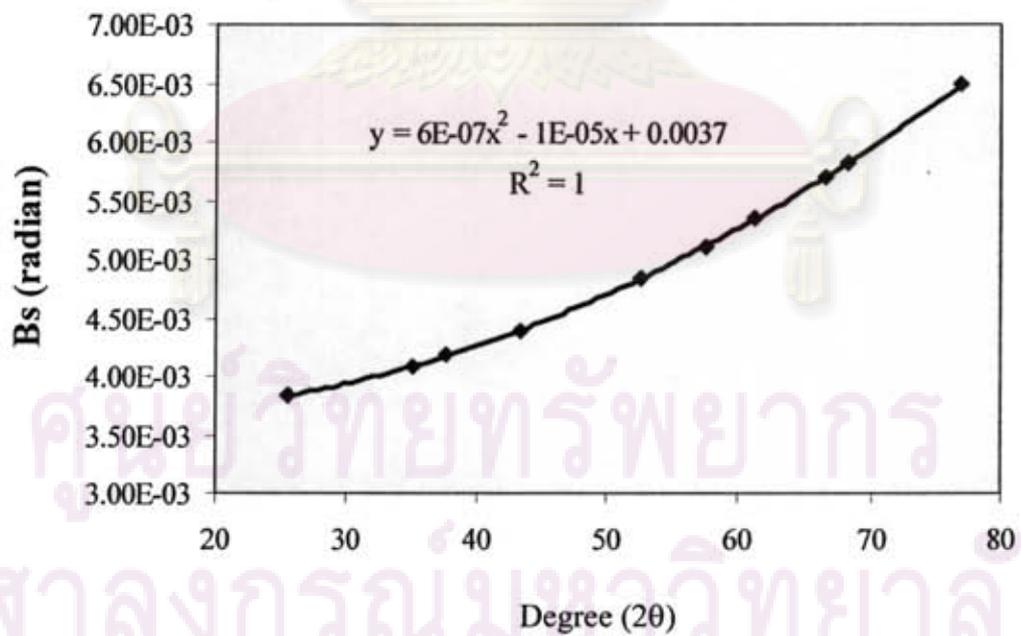
Figure C.2 The plot indicating the value of line broadening due to the equipment. The data were obtained by using α-alumina as standard.

VITA

Miss Sarinee Charoenseri was born on October 1, 1983 in Chachoengsao, Thailand. She finished high school from Datdaruni School, Chachoengsao in 2002, and received the bachelor's degree in Chemical Engineering from Faculty of Engineering, King Mongkut 's University of Technology Thonburi in 2006. She continued her master's study at Chulalongkorn University in June, 2006.